January 2012

A Novel Device and Nanoparticle-Based Approach for Improving Diagnosis and Treatment of pelvic Inflammatory Disease

Natasha Faith Cover
University of South Florida, ncover@mail.usf.edu

A Novel Device and Nanoparticle Based Approach for Improving the Diagnosis and Treatment of Pelvic Inflammatory Disease

by

Natasha Faith Cover

A dissertation submitted in partial fulfillment
of the requirements for the degree of
Doctor of Philosophy
Department of Chemical and Biomedical Engineering
College of Engineering
University of South Florida

Co-Major Professor: Susana Lai-Yuen, Ph.D.
Co-Major Professor: Anna Parsons, M.D.
Arun Kumar, Ph.D.
Karl Muffly, Ph.D.
Donald Haynie, Ph.D.
William Lee, Ph.D.

Date of Approval:
December 12, 2011

Keywords: chitosan, infectious diseases, drug delivery, uterine sampler, medical device

Dedication

This dissertation is dedicated to my family in Jamaica, London, and here in the United States. To my parents, brothers, sisters, and all my friends whose love and support have been immeasurable throughout the years.

"To whom much is given, much is required"

Acknowledgements

With a humble feeling in my heart as I write this acknowledgement, I would first like to thank the Lord, for if it had not been for Him none of this would be possible. Then I want to say a heartfelt thank you to my advisors, Drs. Susana Lai-Yuen and Anna Parsons, and committee member Dr. Arun Kumar for their continuous support, constant encouragement, and guidance throughout the years. This dissertation would not be possible without their intellectual support. Special thank you to my other committee members: Drs. William Lee, Donald Haynie, and Karl Muffly for their excellent guidance. Very special thanks to Dr. Don Cameron for providing the lab space for me to finish up my work. My sincere appreciation goes to Mr. Bernard Batson, Dr. Shehkar Bhansali, and everyone associated with the Bridge to the Doctorate and McKnight Doctoral Programs for their continuous support. I also want to thank my fellow lab members for always being there to answer any question at any time.

True friends come around once in a life and here I am at the age of 28 and have the greatest friends whose encouragement has kept me going my entire five years here at USF. A very love-felt thank you to Nekesha, Regina, Kathryn, LaTia, Al-Aakhir, Phaedra, Shara, and Yvonne. To Pastor Aubrey Shines, Dr. Joan Ganns, and my Glory-to-Glory family: your love, support, and prayers are immeasurable.

Finally, I would like to thank all of my family members for their unconditional love and support throughout this Ph.D. process. A warm-felt thanks you to my grandparents, parents, aunts, uncles, brothers, sisters, and cousins. I love you all.

Table of Contents

List of Tables

List of Figures

Abstract

Pelvic Inflammatory Disease (PID) is one of the most common causes of morbidity in women. PID is a polymicrobial infection of the female reproductive tract, and is associated with pelvic pain, abnormal uterine bleeding, and tubal damage that can lead to ectopic pregnancies and infertility. It is curable but the effects of PID can be permanent if not properly diagnosed and treated. PID presents as a spectrum of disease and is often missed at early stages; even acute PID can be difficult to diagnose, as there is no single conclusive diagnostic test. Currently, PID is identified and treated syndromically because pelvic pain is the only consistent clinical finding. The Center for Disease Control and Prevention (CDC) recommends doxycycline, a broad-spectrum antibiotic, for treatment but doxycycline can cause gastrointestinal irritation and local inflammation leading to an incomplete treatment. Most cases of PID are polymicrobial infections of the tubes and endometrium, which are not accessible to culture due to the difficulty of procuring samples above the naturally contaminated vagina and distal cervix. Given the difficulty of properly diagnosing PID and the limitations and side effects of the current treatments, there is an urgent need for new approaches for improving the accuracy for diagnosis and treatment of PID. We propose a new and practical approach to collect sterile specimen samples from the endometrium for more accurate PID diagnosis, and to treat the reproductive tract locally using doxycycline-loaded nanoparticles. The proposed research presents a novel sterile uterine sampler cover (SUSC) device that can safely and effectively collect uncontaminated specimen samples from the uterus, and also deliver nano-encapsulated drugs directly to the site of

infection. The analysis of uncontaminated endometrium samples is expected to provide an understanding of uterine flora in symptomatic and asymptomatic women, and will lead to the identification of infective microbes in symptomatic women for pathogen-specific treatment. The use of nano-encapsulated doxycycline will enable localized drug delivery to lower drug dosage and minimize side effects for the patient. The doxycycline-loaded nanoparticles are characterized and evaluated based on their drug release properties, size distribution, and tissue response in vitro. This research will lead towards a more effective approach for the diagnosis and treatment of PID while freeing women from prolonged systemic treatments and their adverse effects. Moreover, this research will increase our understanding of the uterine biome under various hormonal and pathologic conditions, in symptomatic and asymptomatic women.

Chapter 1 - Introduction

1.1. Motivation

According to the Centers for Disease Control and Prevention (CDC), an estimated 1.0 million women in the United States experience acute pelvic inflammatory disease (PID), and 1–2 billion dollars are spent for PID and its sequelae treatment each year.[1-6] PID is an infection of the upper genital tract, which includes the uterus (endometrium), fallopian tubes, and surrounding organs. It is hypothesized that microorganisms such as *Chlamydia trachomatis*, *Neisseria gonorrhoeae*, and microorganisms of the vagina's normal flora cause PID.[7-9] Symptoms associated with PID include pelvic pain, abnormal uterine bleeding, and vaginal discharge. The reproductive infection can also result in tubal damage, which can lead to ectopic pregnancies and infertility.[2,4,8,10,11] Unrecognized (dormant) infection is thought to be associated with preterm labor, and neonatal mortality. Approximately 33% of severe PID cases are reportedly incorrectly diagnosed, --a lack of reliable and conclusive diagnostic testing can make detection of acute PID very difficult.[3,12,13] And in its early stages, PID often goes undiagnosed as symptoms can be subtle.[14]

Current PID diagnosis is based on CDC recommended minimal diagnostic criteria: pelvic pain as cervical motion tenderness, uterine tenderness and/or adnexal tenderness.[15] Evidence of lower genital tract inflammation—leukocytes in vaginal secretions, cervical exudates or bleeding on contact--increases the likelihood of PID as a cause for pelvic pain. Other supportive but not necessary findings include: temperature above 38.3°C, an elevated erythrocyte sedimentation rate, elevated serum levels of C-

reactive protein, prior or current *N. gonorrhoeae* or *C. trachomatis* infections, or an inflamed mass on pelvic sonography.[10,13] Along with the CDC criteria, medical history especially risk factors, physical examination, and a few laboratory tests, including C reactive protein, peripheral white cell count, and erythrocyte sedimentation rate, and cervical testing for C trachomatis and N gonorrhea constitute the usual methods for diagnosing PID. The sensitivity and specificity of these laboratory test approaches ranges from for poor to fair when it comes to diagnosing PID.[8,10] It has long been observed that women with no history of recognized PID often present with tubal factor infertility.[16-18] Persistent Chlamydia in the upper reproductive tract was identified in 15% of 52 women undergoing tubal surgery for infertility.[19] Chlamydia was found in the peritoneal fluid in 44% of women laparoscoped for pelvic pain with signs of salpingitis, and in 37% of women undergoing surgery for tubal sterility.[20] Recent data have broadened recognition of subclinical PID (15) as identified by the presence of leukocytes and plasma cells in an endometrial biopsy.[14] However, use of endometrial tissue for microbial identification has not been adequately tested using modern genetic identification techniques. Neither have the normal flora of the healthy uterine cavity been characterized.

Ultrasound is useful for detecting overt inflammatory changes in pelvic organs, but has poor sensitivity when these are minimal.[1,10,21] The current gold standard for diagnosing PID is laparoscopy, a minimally invasive surgery, to provide physical evidence and allow upper tract sampling. However, this is a resource intensive procedure requiring general anesthesia with significant risk.[10,22,23] Empirical antibiotic therapy that covers both *Chlamydia trachomatis* and *Neisseria gonorrhorrhea* is the first line of treatment. The patient is then monitored to determine if or when symptoms subside, while awaiting test results for cervical evidence of Chlamydia or gonorrhea.[1]

The CDC recommends doxycycline, an inexpensive, widely available broad-spectrum antibiotic, which obtains very high drug levels in the pelvic area, as a key component of treatment. However, this drug can cause gastrointestinal irritation when taken orally, and requires a two-week treatment course. Doxycycline may also cause local inflammation when given intravenously. These side effects often result in incomplete treatment. Current gynecological devices for collecting endometrium cannot provide sterile samples, hence the reliance on evidence of inflammation in endometrial biopsies as sole evidence of 'subclinical' upper tract infection in women with minimal pain. Analysis of uncontaminated endometrial tissue is expected to provide an accurate diagnosis of local inflammation and identify the specific organisms causing it, guiding the selection of the best treatment. As is currently done with urinary tract infections, drugs can be started using current assumptions, and corrected as needed after data is available. Equally importantly, uncontaminated endometrial sampling will allow a better understanding of the natural microbial ecology of the uterus under a variety of spontaneous and manipulated hormonal conditions. It is highly likely that biofilms of sessile pathogens exist in the endometrial cavity as they do in the inner ear, bladder, and prostate, and this has enormous implications for fertility and complications of pregnancy.

The lack of accurate diagnostic methods and/or devices has severely limited understanding of PID, particularly those episodes of inflammation which are associated with bowel commensals rather than Chlamydia and gonorrhea, or produce recurrent symptoms, or occur in apparently low risk women. We hope to avoid delayed treatment in atypical cases, and overtreatment when there is no infection. Once pathogens are identified, we believe that local treatment may be more effective than systemic, as is done in dairy cows.[24] Development of a new topical treatment approach requires

reformulation of currently used drugs for minimal toxicity and effective application—ideally transvaginally by the patient herself.

1.2. Dissertation Objectives and Contributions

Given the difficulty of properly diagnosing PID and the limitations and side effects of the current treatments, there is an urgent need for new approaches to improve the diagnostic accuracy and treatment of PID. We set out to: (a) design and validate a new device to collect uncontaminated samples from the endometrium for more accurate diagnosis of PID, and (b) design and analyze the encapsulation of doxycycline into nanoparticles for targeted drug delivery. The objectives of this research are:

1. To design and validate a sterile uterine sampler device capable of collecting sterile samples from the endometrium
2. To analyze the preparatory variables associated with chitosan nanoparticle preparation via the ionic gelation method
3. To evaluate the doxycycline-loaded chitosan nanoparticles *in vitro* for antibacterial activity on *E. coli* cultures and cytotoxicity on normal human ovarian surface epithelial cells

This approach is intended to provide a simple and accurate method of obtaining specimens of uterine, cervical and vaginal flora separately. DNA analysis of the specimens should demonstrate the uterine biome in both symptomatic and asymptomatic women, stratified by treatment and hormonal status. Conventional culture or quantitative analysis of the microbial populations that are identified as well as immune histology may demonstrate infectious agents, as distinct from commensals. New strategies may be then devised for diagnosis, treatment and prevention of reproductive tract infection. Nanoformulation of doxycycline may provide better, targeted therapy with

less toxicity than systemic treatment to reduce the prescribed dosage and side effects associated with the disease's common drug treatments.

The findings described in this body of work have the potential to decrease adverse health consequences and the cost of treatment, thus improving the quality of life of patients suffering from PID. This work can also help to define and compare the vaginal and uterine flora—both infectious (culturable) and vegetative (biofilms)—in asymptomatic and symptomatic women under various hormonal conditions, and it may allow immediate local delivery of an appropriate nano-encapsulated drug. Uncontaminated tissue samples will allow a better understanding of the natural microbial ecology of the uterus, and this improved understanding will impact both gynecological and obstetrical practice.

1.3. Dissertation Outline

This dissertation is organized as follows. Chapter 2 presents an in-depth literature review. Chapter 3 presents the design and development of the proposed sterile uterine sampler device. Chapter 4 focuses on the analysis of the preparation of doxycycline-loaded nanoparticles. Chapter 5 describes the *in vitro* analysis of these nanoparticles based on their function (antibacterial activity) and biological safety (cytotoxicity). Finally, Chapter 6 summarizes the relevant findings of the dissertation and presents recommendations for future directions.

Chapter 2 - Literature Review

This chapter provides some background on current uterine sampling devices. An overview of previous work on targeted drug delivery techniques, nanoparticle preparation, and the drug doxycycline are also presented.

2.1. Uterus Sampling Devices

Devices that can be inserted into the uterus have been developed for endometrial sampling, pregnancy prevention, and other gynecological procedures. Examples include the select cell, transcervical devices, intrauterine devices (IUDs), and curettes. IUDs are small devices implanted into the uterus for a certain period of time to prevent pregnancy by disrupting the uterine wall or slowly releasing hormones.[25-27] The curette is a metal rod with a handle at one end and a loop on the other end that is used to scrape the lining of the uterus during a gynecological procedure called "dilation and curettage.[28] This procedure was considered the gold standard for sampling the endometrium for more than a century.[29,30]

In 1949, Guilbeau et al. proposed a uterine culture technique for sampling the endometrium of postpartum women while avoiding the contaminated cervical and vaginal areas.[31-33] They suggested using a metal tube with a tightly drawn finger cot (which required chemical sterilization for 48 hours) to occlude the distal end of the cervix and prevent contamination during insertion. Once inserted with a stylet beyond the internal os of the cervix, the finger cot was pierced, thus allowing the inner wire loop to

collect the sample. However, this technique was merely described; no data were presented to document its efficacy.

In 1981, Knuppel et al. presented a transcervical device for sampling the uterus.[32] This specimen collection device consisted of a telescoping Teflon catheter that housed a nylon bristle brush attached to a retractable wire in the inner cannula. At the tip of the outer catheter was a plug made of either gelfoam or polyethylene glycol. Upon insertion of the device, the brush was used to push the plug into the uterus to allow the brush to collect the specimen. Leaving the plug in the uterus was a major drawback. A plug made of polyethylene glycol would take a couple of days to dissolve; a plug made of gelfoam could cause a nidus of infection. This device was designed to pass through the contaminated vaginal and cervical area to the uterus for specimen collection. This device does not protect the uterine sample from the contaminated vagina and cervix, and it leaves the plug portion of the device inside the uterus.

Another technique for culturing the uterus was described by Bollinger.[33,34] In this technique, a Teflon sheath with a Teflon plug was used to reach the uterus. Once inside the uterus, the plug was dislodged by an inner cannula to which a syringe was attached for suction of the specimen sample. The accuracy of this approach was not clearly defined due to the fact that the device used for sampling passes through the contaminated areas of the cervix and vagina.

Between 1981 and 1982, Patrick Duff and his team investigated four different endometrial specimen techniques: (1) transfundal aspiration, (2) transcervical brush biopsy through a double-lumen catheter, (3) transcervical lavage through a double-lumen catheter, and (4) aspiration of secretions from the lower uterine segment through a single-lumen catheter.[33] For the transfundal aspiration, an 18-gauge spinal needle preloaded with sterile polyionic solution is used. Once in the endometrium cavity, the solution was injected through the needle and then immediately aspirated back into the

needle. Knuppel et al described the transcervical double-lumen catheter technique.[32,33] For the transcervical lavage, a sterile polyionic solution was injected in the endometrium cavity through an inner catheter passing through an outer catheter. This injection was followed by immediate re-aspiration. For the fourth technique, aspiration of lower-uterine secretions, a catheter was placed 4 cm above the external os of the cervix and a polyionic solution was then injected and immediately re-aspirated. These techniques were all conducted on uninfected women in the Trendelenburg position. It was observed that the brush biopsy and lavage through double-lumen catheter were the most satisfactory techniques for reducing but not preventing cervical and vaginal contamination.

The select cell©, a newer and smaller version of the Pipelle, is another device used to collect endometrial specimens.[29] The select cell, which removes specimens through suction, is made of a clear, long, and flexible polypropylene sheath with an acetal copolymer rod to which a piston is molded. As with the transcervical devices, the specimen collected by the select cell is not protected from the contaminated vaginal and cervical areas during sampling.

Other endometrium samplers and/or techniques have been patented as shown in Table 2-1. However, none of the currently available or patented devices and/or techniques can procure truly uncontaminated specimen samples from the endometrium and surrounding areas. Sterile samples are necessary for a better understanding of not only normal flora in asymptomatic women but also improved understanding and diagnosis of upper genital tract infection in symptomatic women. One of the objectives of this dissertation research is to design and develop a novel sterile uterine sampler cover (SUSC) device to collect sterile specimen samples from the fallopian tubes, uterus, and surrounding areas to improve the accuracy of diagnosis of pelvic inflammatory disease (PID). Once the disease-causing organism(s) are identified, the proper drug treatment

can be recognized. To improve the treatment drug's efficacy, the drug can be encapsulated into nanoparticles for targeted drug delivery. This device can potentially be used to deliver drug-loaded particles via a transcervical route for more localized drug treatment of PID.

Table 2-1: List of some patented uterus sampling devices.

Year	Author(s)	Patent Title	Reference
1973	Binard Dye	Endometrial Sampler	35
1982	Shah	Medical Device for Collecting Body Sample	36
1983	Milgrom	Tissue Collecting Apparatus	37
1984	Kotsifas Wetzel Gilson	Endometrial Sampling Device	38
1990	Neuwirth Bolduc	Intrauterine Cauterizing Apparatus	39
2003	Anapliotis	Device for Taking Biological or Cytological Smear	40
2008	Gruber	Systems, Methods, and Devices for Performing Gynecological Procedures	41
2008	Alderete Castella	Method and Device for Trichomonas Detection	42
2009	Lee-Sepsick Azevedo Currie	Methods and Devices for Conduit Occlusion	43

2.2. Targeted Drug Delivery

Targeted drug delivery is a unique method for delivering a drug to one particular site of the body in an effort to increase the dosage to that specific location and to reduce adverse side effects. There are three main constituents in a targeted drug delivery system: a drug, a targeted site, and a delivery vehicle.[44] The drug can be either chemically conjugated or passively absorbed into the delivery vehicle. The targeted site is dictated by the nature and origin of the disease being treated. The delivery vehicle (the carrier) is of utmost importance, as it must preserve the pharmacodynamic and pharmacokinetic properties of the drug being carried.[44]

To deliver a drug across cell membranes, several vehicle materials can be used—e.g., natural or synthetic polymers, dendrimers, surfactants, or lipids.[45-47] Among the natural polymers, chitosan is widely used in drug delivery applications because it is biocompatible, biodegradable, and possesses a muco–adhesive property that enables its transport across mucosal membranes.[48-55] These properties make chitosan highly desirable for encapsulating drugs to improve their efficiency, delivery, and controlled release, and thereby reduce their toxicity.[48-57]

Chitosan is a cationic linear amino-polysaccharide biopolymer derived from the deacetylation of chitin (figure 2-1), which is naturally found in the exoskeleton of crustaceans.[48,52,54,58-61] When chitosan particles are used to deliver a drug, the patient's body is capable of breaking down the chitosan into non-toxic amino sugars.[62,63] In addition, chitosan particles can be manipulated to achieve both passive and active drug targeting.[44,64]

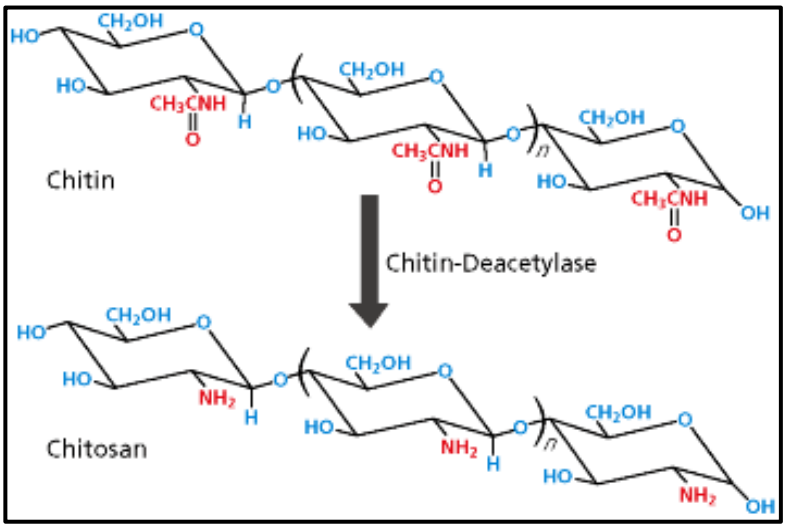

Figure 2-1: The chemical structure of chitin and chitosan.

2.3. Preparation Methodologies for Chitosan Nanoparticles

Encapsulation methods are chosen in part based on polymer properties, drug hydrophobicity, and desired final particle size. The molecular weight of the chitosan plays a vital role in particle size and formation, as a higher molecular weight produces larger particles.[59,65] Another vital component of preparing drug-loaded nanoparticles is the hydrophobicity of the drug.[66] Therefore, the selection of the encapsulation method depends on the desired particle size, drug hydrophobicity, and polymer surface properties to ensure drug encapsulation while minimizing drug loss and maintaining pharmacological activity.

Commonly used methods for preparing chitosan-based drug delivery systems include emulsion cross-linking,[63,66] emulsion-droplet coalescence,[55,63] spray drying,[67] sieving,[63] coacervation/precipitation,[63,66,68] and ionic gelation.[65,66,69-71] Methods such as emulsion cross-linking and emulsion-droplet coalescence involve the use of a harsh crosslinking agent that may induce an unnecessary chemical reaction with the active agents. Spray-drying and sieving produce relatively large microparticles, with diameters of approximately 1–10 μm and 543–698 μm, respectively.[63]

Watzke and Dieschbourg conducted some of the earliest work on preparation of nanoparticles by covalent crosslinking.[72] They prepared chitosan/silica nano-composites by simply reacting tetramethoxysilane with the hydroxyl on the chitosan polymer.[72] At that point, nanoparticle delivery systems were not yet used to encapsulate pharmaceutically active agents (i.e., drugs).[61] Ohya et al. were the first to present data using chitosan nanospheres for drug delivery applications.[60] They used a water-in-oil emulsion method by crosslinking the amino groups of the chitosan with glutaraldehyde to produce nanospheres loaded with 5-fluorouracil, an anticancer drug.[58,60,61,73] Both of these studies demonstrated the preparation of nano-sized particles that can entrap and

deliver drugs.[60] The later discovery of glutaraldehyde's negative impact on cell viability and the integrity of the entrapped drug led to interest in less harsh preparation methods.[60] Ionic gelation is an example of a more benign preparatory method for preparing chitosan nanoparticles.

When chitosan, which is cationic, comes into contact with an anionic compound, it exhibits a unique feature, transitioning from liquid to gel in a process known as ionotropic gelation.[60,61] The first reported case of using ionic gelation for drug encapsulation using TPP as the crosslinker was that of Bodmeier et al.[60,74] This liquid-to-gel process (i.e., gelation) is due to inter- and intramolecular crosslinkages between tripolyphosphate (TPP) phosphates and chitosan amino groups.[60,61] Their aim was to produce chitosan–TPP beads; however, the results were nanoparticles.[60,74]

After the Bodmeier findings, other groups used ionic gelation with TPP as the crosslinker for preparing particles. Shirashi et al. encapsulated indomethacin, an acidic drug, into chitosan gel beads.[75] Calvo et al. looked at encapsulating protein into chitosan nanoparticles.[76] Gan et al evaluated the potential of chitosan nanoparticles for delivering gene or protein macromolecules.[77] Dung et al examined the potential for encapsulating oligonucleotides.[78] Other groups have used ionic gelation to prepare insulin-loaded chitosan nanoparticles.[79,80]

The ionic gelation method has been explored to encapsulate many different biomolecules and drugs, but the linkages between the chitosan and TPP are somewhat weak. To asses this weak linkage, Shu et al explored a novel approach to improving the mechanical strength of chitosan beads.[81] Xu et al later examined different formulations of chitosan nanoparticles prepared by ionic gelation, assessing the effects of the molecular weight and deacetylation degree of chitosan, the concentration of chitosan, and the initial protein concentration.[82]

Ionic gelation is a novel method for preparing chitosan particles, and it offers clear advantages over other methods. Some of those advantages are its simplicity, fast production process, and freedom from a requirement for complicated equipment. In addition, ionic gelation relies not on chemical crosslinking but on reversible physical crosslinking by electrostatic interaction, which reduces the likelihood of the particles' introducing toxins or causing other undesirable effects. The ionic gelation method also offers the flexibility of producing either microparticles or nanoparticles.[83,84]

Despite the significant advantages of the ionic gelation method and the importance of particle size in determining drug-delivery characteristics, definite formulation parameters for producing particles of a specific size range have yet to be defined. In previous work, researchers looked at only one preparatory variable at a time and did not undertake a systematic look at all the preparatory variables simultaneously. The second aim of this dissertation addresses that gap. Our model drug for encapsulation was doxycycline, a commonly prescribed, inexpensive, broad-spectrum antibiotic.[85] In our previous work, we demonstrated that encapsulation of doxycycline into chitosan particles can improve drug delivery and the efficacy of the antibiotic while minimizing adverse effects.[86] The objective of the research was to undertake a systematic study of ionic-gelation preparatory variables and their influence on particle size and morphology. Sixty-four different combinations of chemical constituents and procedural steps were used to generate chitosan nanoparticles of wide-ranging morphology and size. A series of multivariate linear models was constructed to determine the optimum (i.e., most influential) variables for determining particle size. These findings can lay the groundwork for not only understanding but also controlling particle size.

2.4. Doxycycline

Doxycycline is an inexpensive, semi-synthetic antibiotic commonly used as a broad-spectrum drug to treat both intracellular and extracellular bacterial infections. Commonly targeted pathogens include both aerobic and anaerobic gram-positive and gram-negative bacteria and also other microorganisms such as protozoa, mycoplasma, mycobacteria, and spirochetes.[85,87,88] Due to doxycycline's antibacterial effects on a wide range of pathogens, it is currently one of the most commonly prescribed antibiotics worldwide for treating infectious diseases such as pelvic inflammatory disease (PID), a polymicrobial infection.[85,89]

For the treatment of diseases such as PID, the CDC recommends 200 mg of doxycycline to be administrated orally or intravenously every 12 hours.[15] When administered orally or intravenously, however, doxycycline may cause esophageal ulcers, gastrointestinal irritation, and local inflammation, which may in turn lead to premature cessation of treatment.[90-93] Furthermore, the use of doxycycline may result in mechanical scarring of tissues and cavities in the body, as well as blood vessels.[94-98]

In recent years, drug encapsulation and delivery via small particles has garnered increasing interest. Encapsulation may help prevent adverse effects by protecting sensitive tissues from fast drug exposure while also improving drug efficacy by achieving slow, sustained release directly at the infection site. Having patients complete the entire treatment cycle would also increase the likelihood of complete pathogen elimination. These properties suggest that encapsulation of doxycycline into biodegradable nanoparticles could perhaps be used to eventually improve treatment of PID via direct transcervical drug delivery.

We investigated chitosan nanoparticles as a potential carrier of doxycycline. The goal was to undertake an initial assessment of particle properties relevant to

encapsulated drug delivery through a localized (i.e., transuterine) route. We are hoping that introducing doxycycline–chitosan nanoparticles to the reproductive lumen will produce sustained drug levels in the reproductive tract by adhesion of the particles to the mucosa as well as absorption of the particles into the tissue, thus increasing the likelihood of complete pathogen elimination. We created and then characterized doxycycline-loaded chitosan nanoparticles (DCNPs) in terms of their morphology (size and shape), drug encapsulation efficiency and release rates, *in vitro* antibacterial activity, and *in vitro* cytotoxicity.

Chapter 3 - Design of a Novel Sterile Uterine Sampler Cover Device

In this chapter, the design and development of a novel sterile uterine sampler cover (SUSC) device to collect sterile cell samples from the fallopian tubes, uterus, and surrounding areas is presented to improve the accuracy of diagnosis of pelvic inflammatory disease (PID). This device is designed to collect sterile samples from the uterus that can be then analyzed to identify the specific pathogens causing PID as well as other uterine infections. The proposed device can also be used to deliver nano-encapsulated drugs at the site of infection for targeted drug delivery.

3.1. Background

As described previously in Section 2.1, endometrial sampling devices and/or techniques are currently available but none of these devices and/or techniques can procure sterile specimen samples from the endometrium and surrounding areas. Procuring sterile specimen samples is expected to provide an accurate diagnostic of PID and to increase understanding of the normal flora in asymptomatic women.

The SUSC device proposed in this research will enable the collection of uncontaminated endometrium samples through the vagina to increase understanding of the natural microbial ecology of the uterus. The collected samples can be later analyzed to identify the specific pathogens causing PID and to determine adequate treatment methods. The SUSC device can also be used for addressing other gynecological disorders/problems such as removal of obstructions in the fallopian tubes, targeting sperm delivery and delivering MEMs technology containing diagnostic agents for

sensitive imaging of neoplastic cells in the fallopian tubes and monitoring the normal flora of the fallopian tubes and the uterus.

The following sections present the device design and development that include users' requirements, engineering specifications, device design, prototyping, analysis, and validation.

3.2. Materials and Methods

The SUSC device was developed using a formal design process commonly used in medical device development. This formal process began with a discussion of end-user requirements, which led to the corresponding engineering specifications, design concept generation and selection, engineering analysis, device fabrication and validation.

3.2.1. End-User Requirements

A thorough literature review was conducted in combination with a clinician survey (Appendix A) to gather user requirements for a device to collect sterile samples from the uterus. The survey consisted of five short questions that focused on identifying the needs and their importance to determine the specifications of the device. These end-user requirements included: ease of handling; comfortable (to the patient); prevents sample contamination; device durability; and dimensions of the device. The resulting end-user requirements are listed in Table 3-1 in descending order of importance. The importance of each end-user requirements were ranked based on the information gathered from the survey.

Table 3-1: End-User requirements with description of each requirement.

Requirements	Descriptions
Prevent Contamination	Prevents vaginal and cervical contamination from entering the uterus
Patient Comfort	Causes little to no pain during the sampling process
Ease of Handling	It is easy to handle
Device Durability	Device is stiff enough so that it does not bend easily but soft enough that no harm is done to the patient
Dimensions of Device	It is able to be used in cervices of different size

3.2.2. Anatomical Design Constraints

The end-user requirements (Table 3.1) were analyzed and converted to engineering specifications. The SUSC device is designed to enter through the vagina. At the distal end of the vaginal canal, the device enters the uterus through the narrow cervical opening. Therefore, we analyzed the female reproductive system to collect the dimensions and constraints for device specifications. These dimensions vary from woman to woman depending on age and hormonal state; thus the device must accommodate the range of female measurements.

The vagina, where the device enters the body, is connected to the cervix of the uterus (womb). Extending from either side of the uterus are the fallopian tubes, and at the ends of the fallopian tubes are the ovaries, two small almond-shaped organs (Figure 3-1). The fallopian tubes are two thin tubes 80 to 120 mm in length on either side of the uterus that serve as the pathway during ovulation for the egg leaving the ovary to reach the uterus for fertilization. The human vagina is a long, collapsible fibromuscular tubal organ with a length of 60 to 120 mm measured posteriorly. This length varies depending on the age of the female as well as her state of sexual arousal.

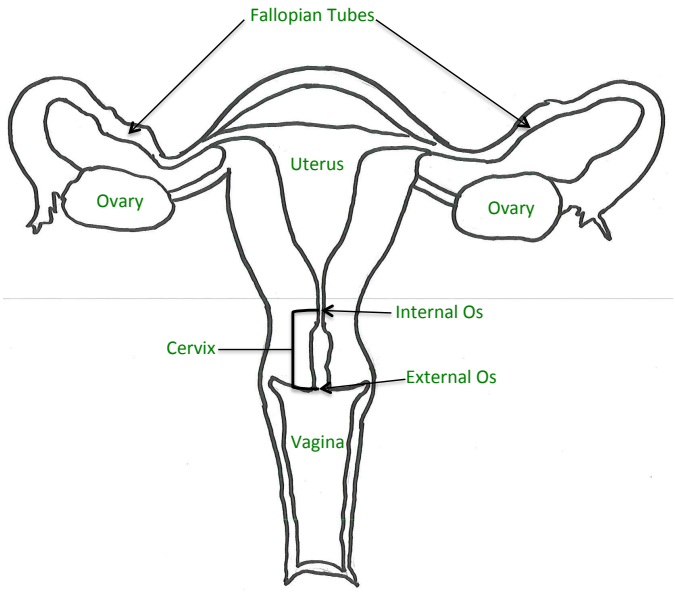

Figure 3-1: Schematic representation of the vagina, cervix, uterus, fallopian tubes, and ovaries.

At the top end of the vaginal tube is the cylindrically shaped cervix, and at the center of the cervix is an opening known as the external orifice (commonly referred to the as "external os"). The portion of the cervix projecting into the vagina is known as the ectocervix and is approximately 30 mm long and 25 mm wide; the dimensions vary depending on age and hormonal state. The spindle-shaped endocervical canal, in the cavity of the cervix, is the passageway between the external os and the uterine cavity; it also varies in width and length. Women of reproductive age have the widest endocervical canals (7–8 mm). The endocervical canal terminates at the internal orifice ("internal os") to the uterine cavity.

If the uterus is cut transversely (Figure 3-2) from the entrance of the left fallopian tube to the right one (A-A') it measures from 26 to 34.6 mm. From the top of the uterine cavity to the internal os (D-D') is 33.2 to 43.8 mm. Going down one-third from the superior portion of the uterine cavity (B-B') is 17.3 to 27.5 mm and then going down

another one-third (C-C') it is 10 to 18.6mm. These dimensions of the endometrium are documented in Chien.[99]

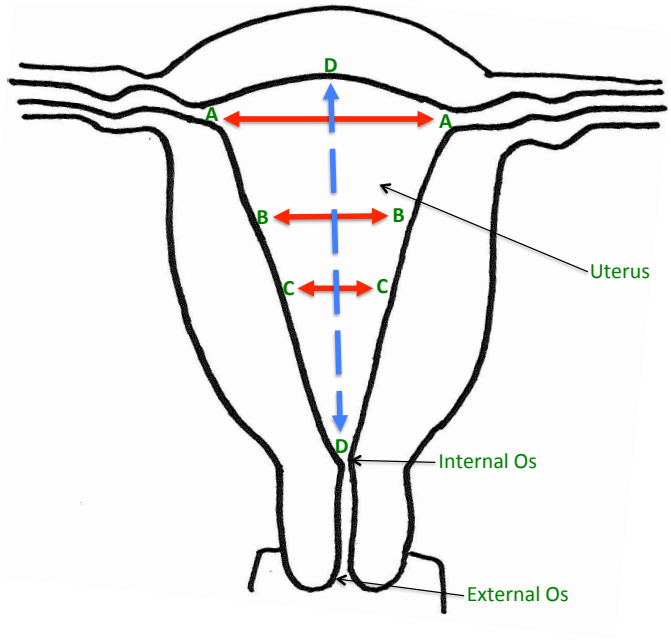

Figure 3-2: Transverse view and dimensions of the endometrium (uterus).

In addition to those dimensional constraints, the positioning of the uterus imposes another constraint. The uterus is normally found in the anteverted position so it is tipped forwards. In a few cases, it is retroverted in the position so it is tipped backwards. The different possible positions of the uterus are illustrated in figure 3-3.

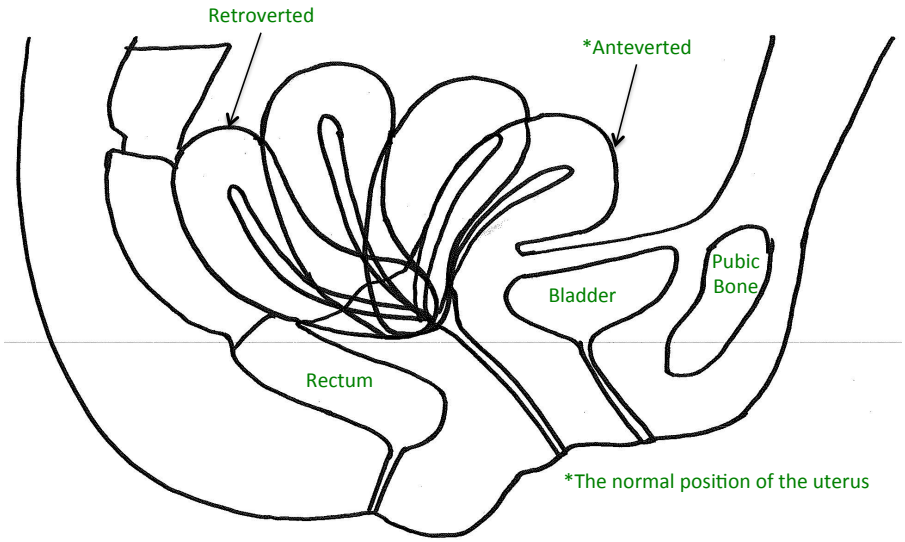

Figure 3-3: Illustration of the different positions of the uterus.

The SUSC device was designed to enter through the vagina, which varies in length from 60 to 120 mm. At the distal end of the vaginal canal, the SUSC device enters the uterus through a 2-3 mm cervical opening. These dimensions vary from woman to woman depending on age and hormonal state. Therefore, the device must accommodate the range of female measurements. Figure 3-4 illustrates the different sizes of the uteruses in different woman at different hormonal stages.

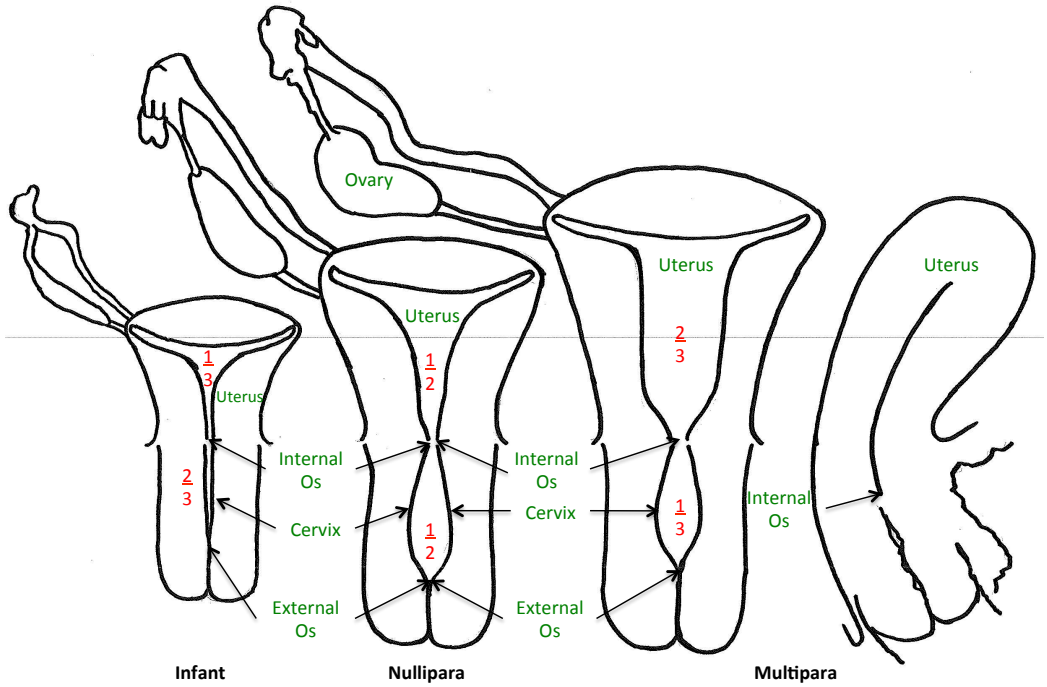

Figure 3-4: Illustration of the uterus at different age groups.

3.2.3. Concepts Generation/Selection and 3D Model Development

After end-user requirements were established, the possible range of device functions was narrowed to two primary aims. The first function of the device is to collect sterile specimen samples from the uterus while preventing vaginal and cervical contamination. The second function is to deliver nanoencapsulated drugs directly to the uterus. Once these primary functions were established, various design concepts were brainstormed and studied. The top three concepts were then evaluated in detail and weighted values were assigned to each end-user requirement and/or function (Table 3-2).

Table 3-2: Detailed evaluations of the top three design concepts arising from the initial brainstorming and preliminary evaluations. The weighted percentage was determined by a survey administered to a group of Physicians.

	Concepts					
	A-Straight One-Sided Sampler		B- Rounded Two-Sided Sampler		C- One-Sided Sampler with Cover	
Selection Criteria/ (Weight)	Rating	Weighted Score	Rating	Weighted Score	Rating	Weighted Score
Prevent Contamination (40%)	1	0.08	2	0.16	5	0.4
Patient Comfort (26%)	3	0.156	2	0.104	4	0.208
Ease of Handling (18%)	4	0.144	2	0.072	4	0.144
Device Durability (10%)	3	0.06	4	0.08	3	0.06
Dimension of Device (6%)	4	0.048	1	0.012	4	0.048
Total Score	0.488		0.428		0.86	
Rank	2		3		1	
Continue?	No		No		Yes	

For the straight single cannula sampler (concept A in Table 3-2), the entire design was a single and straight sampler with an exit hole on the tip of the cannula. The major drawback of this concept was the lack of proper prevention of vaginal and cervical contamination during sampling. In addition, the straightness of this design concept posed another problem. Because the uterus is normally positioned anteverted, insertion of a straight device would have a strong possibility of causing tissue damage. Furthermore, having the exit hole at the tip of the sampler may result in blockage by tissue thus obstructing the sample collection.

The concept of rounded two-sided sampler (concept B in Table 3-2) was also explored. In this design concept, there were two tubes in one barrel. The barrel has two

exit holes that are in opposite direction to allow the inner tubes to emerge for sample collection. The two inner tubes provide dual functionality: suctioning uterine tissue specimens and delivering therapeutic drugs directly to the uterus. The tip of the barrel is rounded to diminish the likelihood of potential tissue damage during insertion. Putting the holes on the side of the device addressed the problem with tissue blockage (as in concept A) upon insertion. Because of the complexity of the internal design, the outer diameter of the barrel would be larger than the single cannula design (concept A). Therefore, this design has a greater potential for causing patient discomfort. In addition, the device does not completely address the prevention of contamination during uterine specimen sampling.

The concept of an outer cannula with a protective cover (concept C in Table 3-2) was also explored. This approach addresses the major problem of contamination, which the other two concepts did not address satisfactorily. The protective cover serves as an outer covering to help prevent the spread of contamination from the vagina and uterus. The outer cannula would provide additional protection from contamination. This design concept has a 20° angle at the distal end of both cannulas, designed to allow the device to follow the normal curvature of the uterus. This overall concept allows for easier insertion and higher prevention of cross contamination.

After evaluation of the designs, concept C was selected for development. Based on the dimensional constraints of the female reproductive system and the proposed function of the device, the device should consist of three components: a sterile cover, an outer cannula, and a sampler. These three components were selected for the final design placing a high priority in preventing contamination while minimizing the outer diameter of the device to reduce any form of pain during insertion. When all three components are assembled, the device's maximum length and diameter should be at least 420 mm and at most 5 mm, respectively. This length ensures its ease of use and maximum distance

from the patient's vaginal area to the external working area. An outer diameter of 5 mm is the absolute maximum to ensure little to no patient pain. The diameter of the sampler should not be greater than 2.5 mm. Table 3-3 summarizes the engineering specifications based on the dimensional constraints imposed by the female anatomy.

Table 3-3: Engineering specifications for each component of the SUSC device.

Part(s)	Function	Dimensions
Outer Cannula	Housing for the sampler	Length = 200 mm Outer diameter = <5.mm Diameter of hole = <3.mm
Sampler	Collect tissue sample and/or to deliver drugs	Length= 240 mm Diameter= <2.5 mm
Sterile Cover	Protective covering of the device	Length= <180 mm

3.2.4. Engineering Finite Element Analysis

Once a design concept was selected and a detailed Solidworks CAD model was developed, finite element analysis (FEA) was used to analyze the design, guide the selection of construction materials, and identify potential failure design points. The amount of bending and deformation of the outer cannula and sampler under stress and/or applied load was analyzed.

3.2.5. Concept Validation

After the failure points of the design model were identified and the design was adjusted, a physical prototype was developed to test the device's primary function: ability to collect sterile uterine samples. The device was named sterile uterine sampler cover (SUSC). The SUSC device was fabricated using polyethylene tubing for the outer cannula, a current endometrium sampler, and latex finger cot for protective cover. The prototype was tested using a Luria-Bertani (LB) agar test. In a test tube, there were two layers of LB agar, the bottom layer was sterile and the top layer was enriched with

Escherichia coli (ATCC 25922). Then, 8 mL of LB agar media was placed in four 15 mL BD Falcon tubes (BD Biosciences), and then allowed to solidify at room temperature. Next, each tube was inoculated with 1.0×10^5 colony-forming units (CFUs)/mL of *Escherichia coli* cells before one hour of incubation at 37°C.

The fabricated prototype device was then used to collect an agar sample from the sterile bottom layer within the test tube. The collected sample was released into another tube containing 4 mL of sterile LB broth. This tube was then incubated at 37°C under light agitation for an hour. After the incubation period, 500 µL of the liquid culture was analyzed at OD_{600} and the number of bacterial cells was calculated. Then, a 100-µL sample of the liquid culture was plated in triplicate on LB-agar plates incubated at 37°C overnight. The controls were as follows: (1) a swab of bacteria from the contaminated layer, (2) sampling with only the sampler and (3) sampling with the sampler passing through the outer cannula without the finger cot. The rationale behind this test was to ensure that the SUSC device could collect a sample of the sterile bottom-layer agar despite passing through the highly contaminated environment of the upper agar layer.

3.3. Results and Discussion

3.3.1. Design Concepts and Prototypes

The SUSC device prototype was designed and analyzed based on the outer cannula with a protective cover (concept C, table 3-2) design. This prototype device has three main components: an outermost protective cover, an outer cannula, and a sampler (figures 3-5, 3-6, and 3-7). The outermost protective cover, made of latex, can be stretched to a maximum length of 180 mm to give maximum elastic stretch at the tip of the outer cannula, thus making it easy to break by the sampler just before sampling. The outer cannula, which houses the sampler, has an outer diameter of 5 mm, an inner diameter of 3 mm, and a wall thickness of 2 mm. On the top of the outer cannula is a 3-

mm in diameter exit hole for the sampler to pass through to collect the samples. The sampler is 240 mm in length, 2.5 mm in diameter, and has a wall thickness of 1 mm. There is a 1-mm diameter hole on the side of the distal tip of the sampler. Tissue samples are drawn through this hole and into the sampler by using the attached plunger to create a vacuum. Each component of this SUSC device, with the exception of the outer protective cover, has a 20° angle at each end to facilitate insertion through the vagina. This design satisfies the engineering specifications: the end-user requirements for the design along with all the anatomical constraints of the female anatomy were addressed.

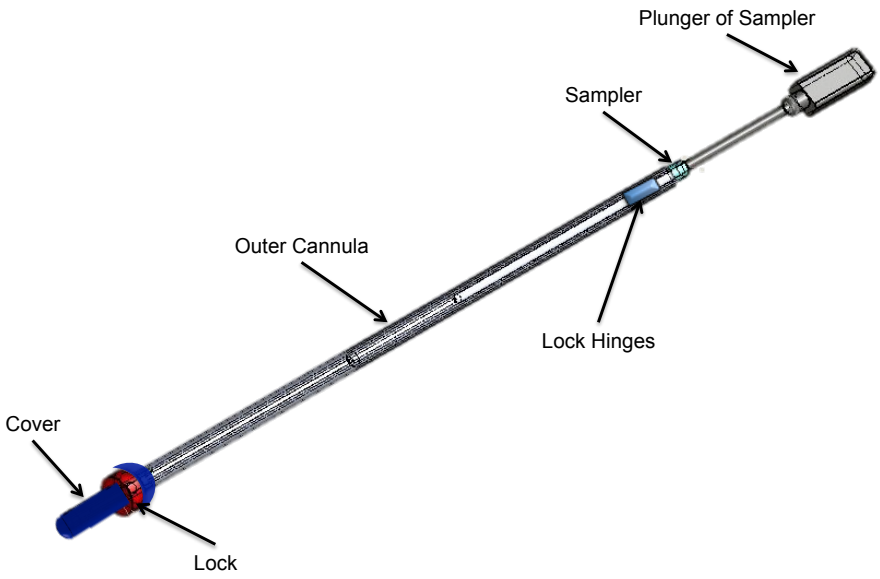

Figure 3-5: The CAD image of the SUSC device.

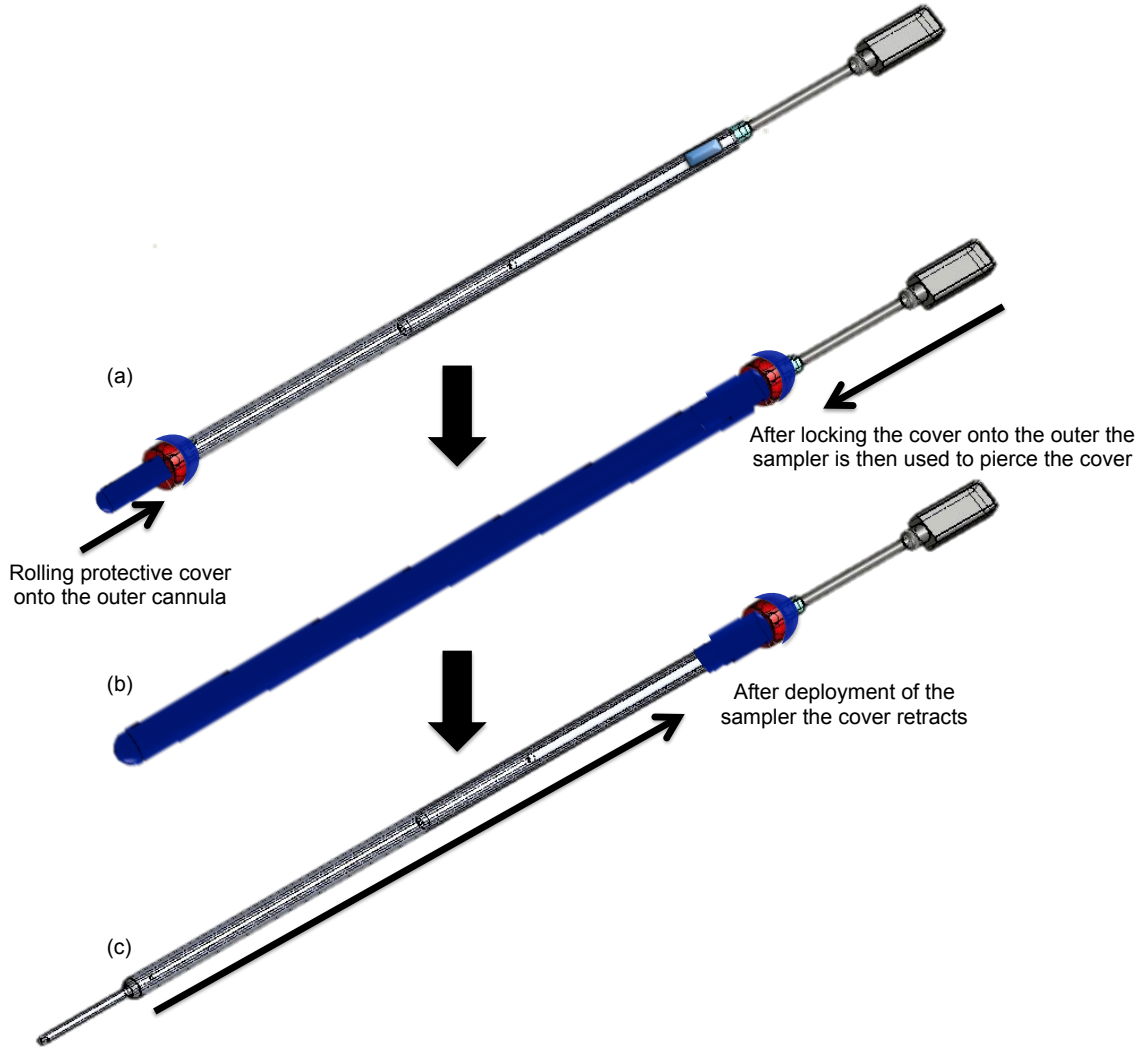

Figure 3-6: The CAD images of the SUSC device showing three different phases. (a) Assembling of the SUSC device (b) the sterile cover stretched and locked in position on the outer cannula and (c) the cover in its retracted position after piercing with the sampler.

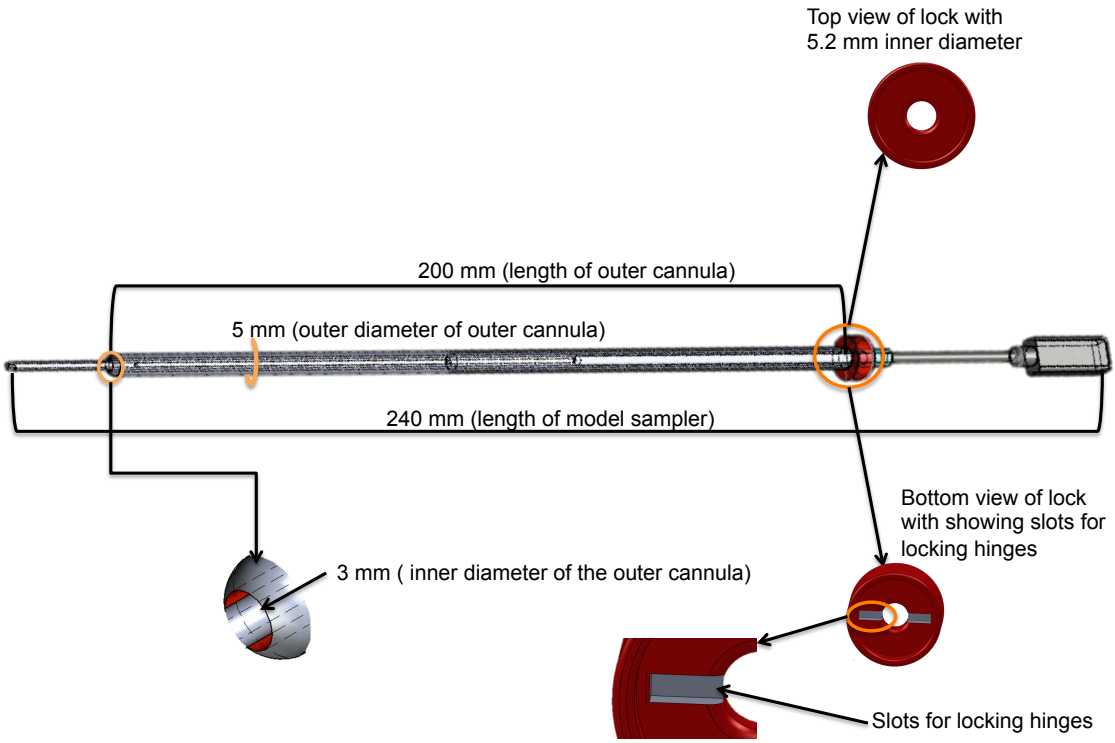

Figure 3-7: The dimensions of the SUSC device.

3.3.2. Deformation and Stress Distribution

To simulate insertion of the device into the vagina, a 1N force was applied to the device components, and the resulting bending and deformation was measured. The first simulation was for testing the potential bending of the outer cannula during insertion in the vagina. The second simulation was for testing the ability of the sampler to break the stretched protective cover on the outer cannula before sampling. Figure 3-8(a) shows the stress distribution after applying a 1-N force to the external end (the end not being inserted into the vagina) of the outer cannula made of a low-density polyethylene (PPE). This simulates the force applied on the outer cannula by the stretching of the protective cover. Figure 3-8(b) shows the results for a 1-N force applied to the sampler to simulate the force associated with breaking the protective cover.

The red areas indicate the most stressed areas while the blue areas are the least stressed. For this particular simulation, the outer cannula experienced no areas of critical stress (the image shows no red areas). On the other hand, the tip sampler, which is used to break the protective cover, is under critical stress, evidenced by the red areas. Still, the component was not deformed. Therefore, both the outer cannula and sampler are expected to withstand the forces caused by stretching the protective cover and breaking the protective cover. In both cases, the yield strength (the stress which the material deformed plastically) of the low-density polyethylene was 6,894,757.3 N/m^2. Based on the applied force, the maximum stress for the outer cannula was 404,763.1 N/m^2; for the sampler, 13,163.3 N/m^2.

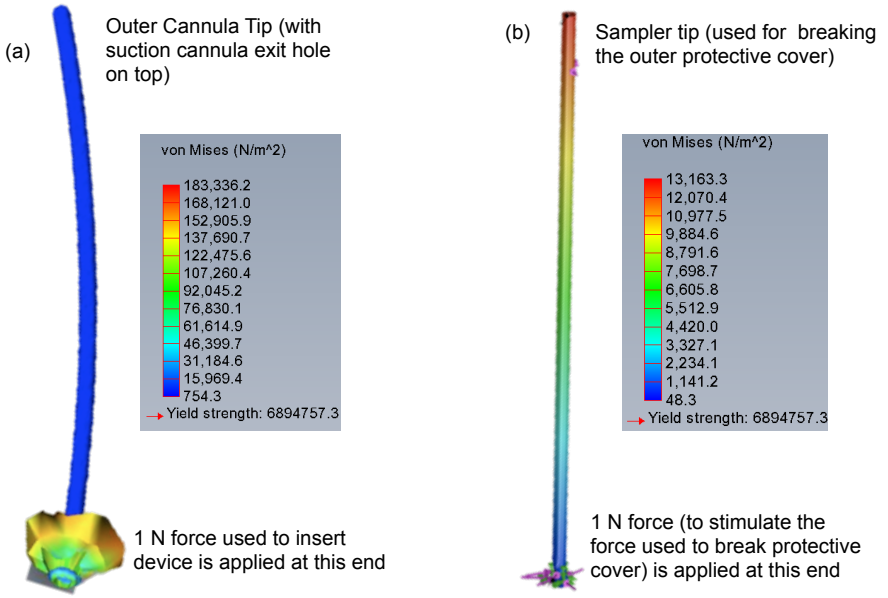

Figure 3-8: The FEA images illustrating the stress distribution. A 1-N force was applied to (a) outer cannula and (b) sampler with low-density PPE as the test material.

3.3.3. Device Operation and Sterile Sampling

This medical device should be used only by licensed gynecological healthcare providers in a sterile clinical setting. Following are the proposed steps for operating the SUSC (Figure 3-9): The lubricated sterile protective cover is pulled toward the operator and locked so that it covers the cannula completely. The SUSC device is then inserted through the vagina through the previously cleansed cervix until it reaches the internal os. Given the diameter of the cannula, there will be resistance at the internal os and this location will be clearly felt by the user. Once the cannula is positioned at the internal os, the protective cover is stretched on the body of the outer cannula and the sampling device is advanced until the protective cover breaks and retracts to the lock, outside the vagina. The sampling device can then enter into the uterus for endometrial collection. The sampling device is then removed from the uterus and the specimen is deposited into sterile media for culture or genetic analysis.

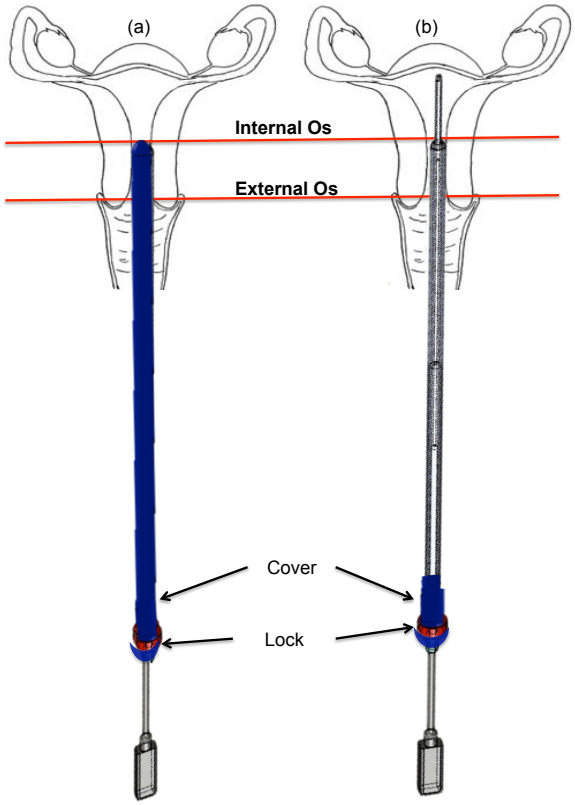

Figure 3-9: Illustration of the operation of the SUSC device. (a) SUSC insertion with protective cover in the lock position on the outer cannula, and (b) sampler deployment and protective cover retraction.

The SUSC device and three different sampling methods were tested to analyze the effectiveness of the device. These three sampling methods were: use of a swab, use of a sampler only, and use of a sampler inside an outer cannula. When using the different approaches to sample a sterile agar layer confined beneath an upper contaminated layer, the SUSC device resulted in much lower sample contamination as shown in Figure 3-10. Compared to a swab from the contaminated layer (100% contamination), using a bare sampler to penetrate the upper layer and sample the lower sterile layer resulted in a 27% reduction in contamination. Using a sampling device in an outer cannula (no protective cover) resulted in only a 7% reduction in contamination. In contrast, sampling with the SUSC device resulted in 92% reduction in contamination.

These percentages were obtained by analyzing liquid cultures using optical density at 600 (OD_{600}). It is believed that the level of contamination on the sample, although minimal, could be the result of human error during sampling and that further practice in using the device would help to decrease this contamination. Compared to the plate streaked with a sample of the contaminated layer (Figure 3-11(a)), the plates streaked with samples from the sampler only (Figure 3-11(b)) and the suction device in the outer cannula with no protective covering (Figure 3-11(c)) show similar confluent bacterial overgrowth. On the other hand, only a few isolated colonies were observed on the plates streaked with samples from the SUSC device as shown in Figure 3-11(d).

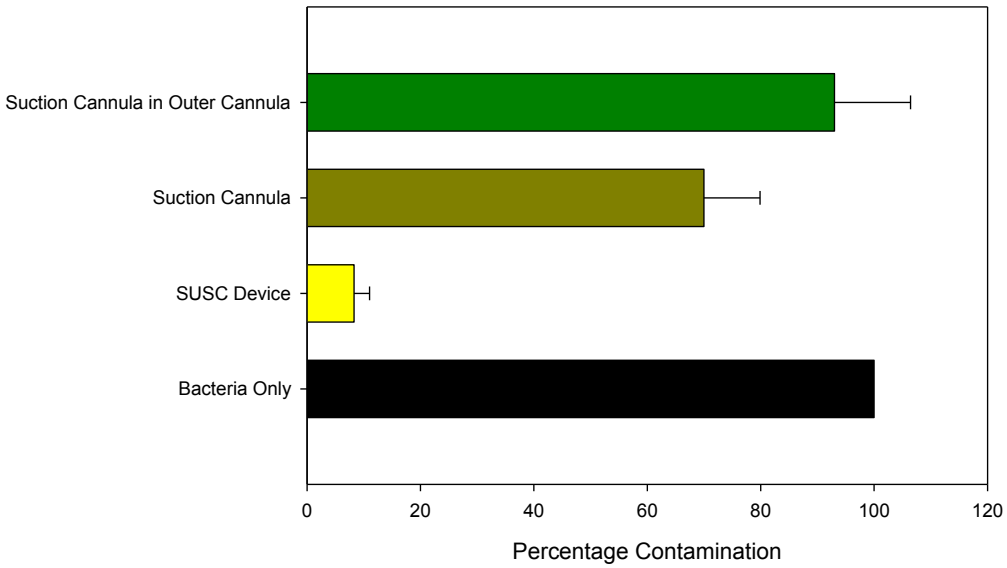

Figure 3-10: Specimen contamination resulting from various techniques used to sample a sterile agar layer confined beneath a contaminated upper layer.

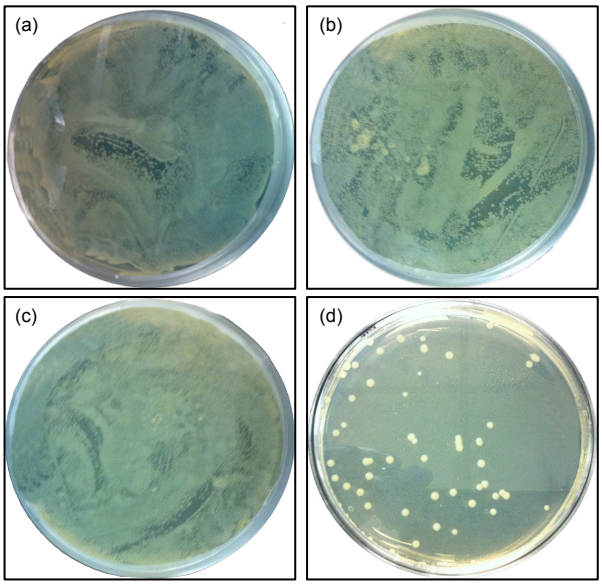

Figure 3-11: LB-agar culture plates for samples collected from a sterile agar layer confined beneath a contaminated upper layer. Collection techniques: (a) no technique; swab from the *E. coli*–contaminated upper layer, (b) sampler only, (c) sampler in outer cannula (no protective covering), and (d) the proposed SUSC device.

3.4. Summary

In this chapter, a single-use sterile uterine sampler cover (SUSC) device for collection of uncontaminated uterine specimen samples for a more accurate diagnosis of PID and other endometrial infections was presented. The SUSC device consists of three components: an outermost protective cover, an outer cannula, and a sampler. The protective cover of the SUSC device aims to protect the device during insertion through the naturally contaminated vagina and cervix for the collection of uterine specimens. The main advantage of the presented device is that its protective cover and sterile technique can be used with any currently available endometrial sampler with an outer diameter of up to 3mm, such as the Pipelle, Explora curette or select cell©. Once the SUSC device is in place, a delivery cannula could be inserted into the uterus for delivery of nano encapsulated drugs to the uterine cavity for treatment of infection. The next chapter will

present the analysis of twelve selected preparatory variables of the ionic gelation method for encapsulating an antibiotic into chitosan nanoparticles. These antibiotic-loaded chitosan nanoparticles can then be transvaginally delivered using the SUSC device for potential treatment of PID.

Chapter 4 - Analysis of Preparatory Variables Relevant to Chitosan Particle Formation by Ionic Gelation

This chapter presents a systematic study of the preparatory variables of the ionic gelation method and their effect on the chitosan particles' characteristics. In the study, multivariate analysis is used to determine the optimum model of preparatory variables that influence particle size. The variables selection was performed using multiple regression analysis through two methods: Akaike's information criterion (AIC) and F-statistics/p-value selection methods. This optimal model can increase understanding of particle size formation using the ionic gelation method to enable mass production of particles of desired size for drug delivery systems.

4.1. Background

Chitosan particles have been extensively explored as a promising drug delivery system due to their muco-adhesive property, which is of great value for delivering particle-encapsulated drugs to intracellular sites. As described in Chapter 2, the ionic gelation method is one of the most commonly used methods for preparing these particles. However, previous work only studied one preparatory variable at a time, and did not provide a systematic analysis of all the preparatory variables at once. The aim of this study is to identify the most relevant methodological parameters in determining chitosan particle size to control particle formation for particular delivery systems.

The particles were characterized in terms of their morphology and particle size distributions. Two statistical selection methods were applied to these data to build an

optimal model: Akaike's information criterion and F-statistics/p-values selections. These statistical analyses were used to identify preparatory variables that were statistically significant in determining the average diameter of the chitosan particles. The analysis of the preparatory variables lays the groundwork for a better understanding of chitosan particle size variation when synthesized by the ionic gelation method. This can potentially lead to better control of particle size formation to enable the mass production of chitosan particles using the ionic gelation method for specific drug delivery systems.

4.2. Materials and Methods

4.2.1. Materials

Chitosan powders (deacetylation of 75%) were obtained from Sigma Aldrich (USA). Sodium tripolyphosphate (TPP) powder was supplied by Sigma Chemical Company (USA). Doxycycline, phosphate buffered saline (PBS), and acetic acid were obtained from Fisher Scientific (USA). All other chemicals were of analytical grade and were obtained from a variety of vendors.

4.2.2. Preparation of Chitosan Nanoparticles

Chitosan particles were prepared using the ionic gelation method of Clavo *et al*.[70] The basic procedure entailed mixing the polymer with a crosslinker to prepare blank (no-drug) particles. For drug-loaded particles, doxycycline was added to the mix as shown in Figure 4-1. Sixty-four different formulations that consisted of different combinations of chemical constituents and procedural steps were used to create the chitosan particles (table 4-1). In earlier experiments done by our group, the effect of using a wider range of acetic acid concentrations (0.25M, 0.50M, and 0.75M) to dissolve the chitosan powder was also evaluated.

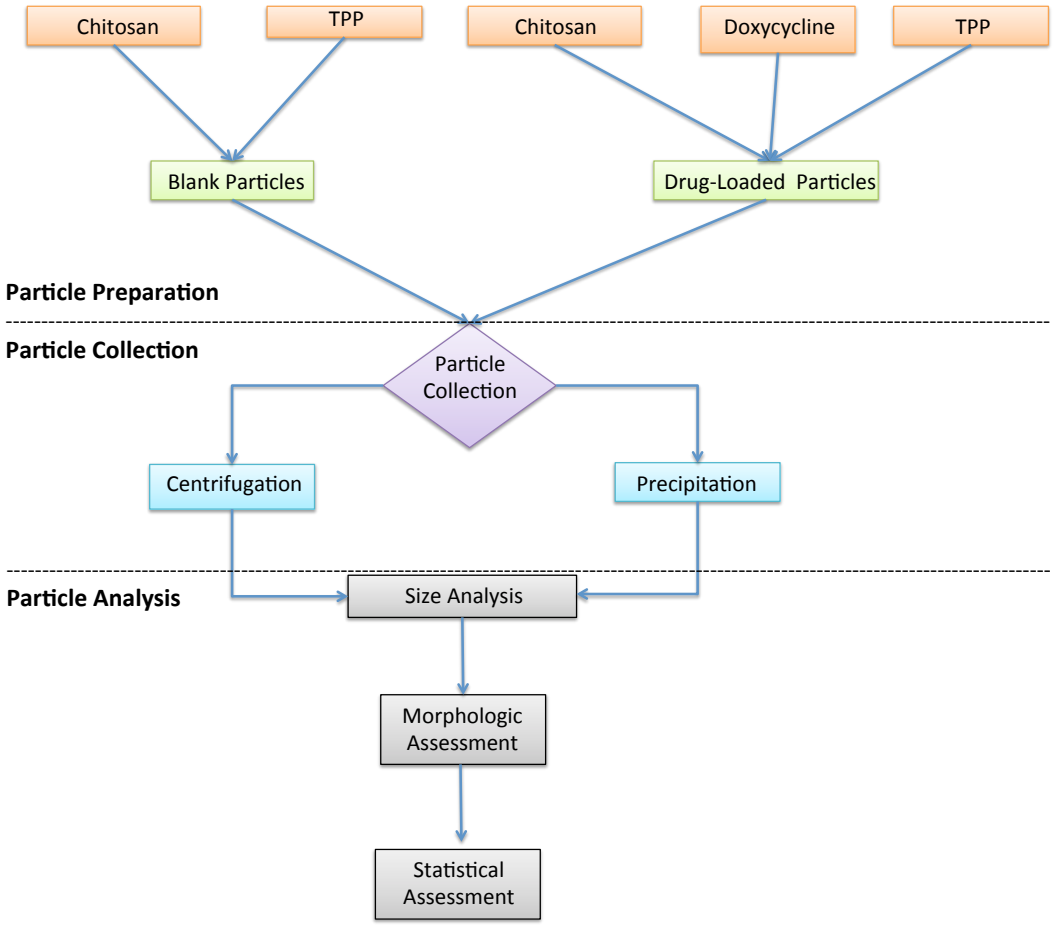

Figure 4-1: Schematic representation of the variables involved in the overall process for preparing chitosan nanoparticles.

Table 4-1: List of variables and values used in the formulation of the chitosan nanoparticles.

Variable	Symbol	Values				
Chitosan Type	X_1	10 kDa			60 kDa	
Chitosan Concentration	X_2	0.1 w/v%			0.2 w/v%	
Chitosan Dissolving Solution	X_3	Water			Acetic Acid (0.25M)	
Chitosan Protonation Time	X_4	1 hour			24 hours	
TPP Concentration	X_5	0.21w/v%	0.42w/v%	0.60w/v%	0.75w/v%	0.84w/v%
TPP Dissolving Solution	X_6	Water			Acetic Acid (0.25M)	
Drug	X_7	Doxycycline			None	
Order of Combination	X_8	Chitosan + Doxy + TPP			TPP + Doxy + Chitosan	
Chitosan: TPP Ratio	X_9	1:2		1:4		1:6
Synthesis Time	X_{10}	1 hour		2 hours		24 hours
Centrifugation	X_{11}	Yes			No	
Wash/Reconstitution Solution	X_{12}	Water			PBS	

Chitosan solution was prepared by dissolving the chitosan powder—10 kDa or 60 kDa (Table 4-1, variable X_1)—in acetic acid or water (X_3) for a final concentration (variable X_2) of 0.1% or 0.2% weight by volume (w/v). This solution was magnetically stirred at 400 rpm at room temperature and allowed to protonate for 1 hour or 24 hours (variable X_4). The cross-linker, sodium tripolyphosphate (TPP), was prepared by dissolving it in acetic acid or water (X_6) to achieve final TPP concentrations ranging from 0.21% to 0.84% w/v (X_5). The various combinations of chitosan and TPP concentrations produced three different chitosan:TPP ratios (X_9): 1:1, 1:2, 1:3, 1:4, 1:5, 1:8, 3:1, and 6:1.

Some particles were prepared as blanks that contained no drug, and other particles were prepared to encapsulate the model drug, doxycycline (Table 4-1, variable X_7). Doxycycline stock solution (200 mg/mL) was prepared by dissolving doxycycline powder

in nanopure water. To initiate ionic gelation (particle formation), the chitosan, TPP, and drug solutions were combined (Figure 4-1). Blank nanoparticles were formed by dropwise addition of TPP to a chitosan solution that was being magnetically stirred. Drug-loaded particles were formed by dropwise addition of 100 µL of doxycycline to the chitosan solution before dropwise addition of TPP, or by dropwise addition of doxycycline to a stirred TPP solution before dropwise addition of chitosan (variable X_8). The blank and drug-loaded solutions were allowed to synthesize particles for 1, 2, or 24 hours (X_{10}) under magnetic stirring at room temperature. The particles were then collected and were centrifuged at 10,000 rpm for 5 minutes or were allowed to precipitate at room temperature until supernatant is clear and pellet is obvious (X_{11}). The resulting pellet or precipitate was then washed and resuspended in either nanopure water or phosphate buffered saline, PBS (X_{12}).

4.2.3. Physical Characterization of Nanoparticles

Particle size distributions were determined with a Microtrac Particle Size Anaylzer (measures particles sizes from 0.8 to 6500 nanometers), which measures dynamic light scattering by particles. All analyses were performed on samples diluted in 1 mL nano-pure water. Morphology of the chitosan nanoparticles was examined using a JEOL 1400 transmission electron microscope (TEM). TEM samples were prepared by placing a drop of resuspended nanoparticles (blank or drug-loaded) onto a formvar-coated copper grid that was allowed to dry before TEM analysis.

4.2.4. Variable Selection

To quantitatively assess and determine which of the twelve preparatory parameters (table 4-1) had the greatest influence on particle size, a series of multivariate linear models were constructed. Multivariate linear regression modeling is an approach used to model the relationship between a dependent variable and several independent variables.[100] The models were then ranked using Akaike Information Criterion (AIC) and F-statistics/p-value methods. Both methods are independent from the distribution of the variables; in other words, both work well for normal and non-normal data distributions. The twelve preparatory variables investigated, X_n, are listed in table 4-1; average particle diameter, Y, was the dependent variable. All statistical analyses were performed using MATLAB (version 2009b).

The AIC selection approach builds the simplest possible optimal model to explain observed variation in an experimental outcome,[101-104] which in our case is the mean particle diameter Y. The method performs stepwise selection of significant preparatory variables through forward addition based on the AIC value, which measures how much variation in outcome, Y, can be accounted for by each individual variable. AIC considers the number of observations (n); the number of explanatory variables (K) and the residual sum of squares (RSS) for each model and the AIC value is calculated based on equation 1.[102,103]

$$AIC = n \bullet \log_e(RSS/n) + 2K \qquad (1)$$

The F-statistics/p-value variable-selection method, like the AIC-based method, also builds an optimal model based on the empirical data set—identifying those variables that exert the greatest influence on particle diameter—but does so by selecting variables with significant p-value for the final model. This non-parametric, permutation-based method assesses each variable's statistical significance and its influence on the variation in the

outcome, Y, before selecting it to the final model. Variables are sequentially added by selecting the variable that yields the largest partial F-statistic with significant p-value and corresponding adjusted R^2.[102] To test the significance of each variable in the model, an *F*-statistics test was performed using a level of significance, alpha (α), of 0.05.

Conditional tests were conducted for both selection methods to first examine the independent effect of each preparatory variable on mean particle diameter. For AIC-based selection, the conditional test is used to select the order of variable entry into the final model. Marginal tests, in contrast to the conditional tests, examine the effect of each variable on Y after taking into account the effects of preparatory variables previously selected during the stepwise variable-selection procedure.

4.3. Results and Discussion

4.3.1. Statistical Selection of Influential Preparatory Variables

The AIC-based variable-selection method identified four of the twelve variables as substantially contributing to variation of mean particle diameter (Y): chitosan-to-TPP ratio (X_9), wash/resuspension solution (X_{12}), synthesis time (X_{10}), and TPP concentration (X_5). Conditional testing was conducted first to assess the independent effect of each of the twelve preparatory variables and to select the first variable to enter in the final model (table 4-2). A variable's AIC value is of great importance because it expresses the strength of the variable's influence on particle size variation: the smaller the AIC value, the more of the Y variation that is explained. Each variable has an AIC value, which is assigned a corresponding weight (Wts). The variable with the lowest AIC value was assigned a weight of zero and the remaining weights were scaled accordingly.

Table 4-2: Results of the conditional test using the AIC-based stepwise forward selection. Variables selected to be in the final model are shown in bold.

Variables	AIC	Wts	R^2	R^2adj
Chitosan:TPP Ratio, X_9	**952.4053**	**0**	**0.3105**	**0.2994**
Chitosan Type, X_1	963.4904	11.0851	0.1802	0.1669
TPP Concentration, X_5	**971.2121**	**18.8068**	**0.0750**	**0.0601**
Chitosan Concentration, X_2	972.0659	19.6606	0.0626	0.0475
Wash/Resuspension Solution, X_{12}	**972.3683**	**19.9630**	**0.0582**	**0.0430**
Chitosan Dissolving Solution, X_3	972.8854	20.4801	0.0505	0.0352
TPP Dissolving solution, X_6	974.4036	21.9983	0.0277	0.0121
Order, X_8	975.5816	23.1763	0.0097	-0.0063
Protonation Time, X_4	976.0933	23.6880	0.0017	-0.0144
Drug, X_7	976.1125	23.7072	0.0014	-0.0147
Synthesis Time, X_{10}	**976.1614**	**23.7561**	**$6.6606e^{-04}$**	**-0.0155**
Centrifugation, X_{11}	976.2040	23.7987	$5.0692e^{-07}$	-0.0161

Table 4-3 shows the variables selected for the optimal model selected by the AIC method. The variables selected for inclusion in this final model may not have had the lowest AIC values in the conditional testing of each individual variable (table 4-2) but together in the final model they resulted in the lowest cumulative AIC value (table 4.3). In this case, R^2 values correlate well with the AIC values within the final model, which can explain 58% of the total variation in particle diameter.

Table 4-3: List of variables selected for inclusion in the optimal model using the AIC-based selection method.

Variables	AIC	Wts	R^2	R^2adj
Chitosan: TPP Ratio, X_9	952.4053	0.9958	0.3105	0.2994
Wash/Resuspension Solution, X_{12}	938.3569	0.8535	0.4652	0.4476
Synthesis Time, X_{10}	930.1306	0.7613	0.5461	0.5234
TPP Concentration, X_5	928.1074	0.2282	0.5761	0.5474

The F-statistics/p-value stepwise method selected the same four variables as being significant in contributing to variation in particle diameter for the optimal model (table 4-4). As with the AIC-based method, conditional testing on each of the twelve variables was conducted first. The fact that both methods selected the same four variables for the optimal model (tables 4-3 and 4-4) is a strong indication of the significance of these variables in determining mean particle diameter.

Table 4-4: List of variables selected for inclusion in the optimal model based on the F-statistics/p-value selection method.

Variables	Partial F	P	Partial R^2	Partial R^2 adj
Chitosan:TPP Ratio, X_9	27.9262	$1.0000e^{-03}$	0.3105	0.2994
Wash/Resuspension Solution, X_{12}	17.6342	$1.0000e^{-03}$	0.1546	0.1410
Synthesis Time, X_{10}	10.7019	0.0030	0.0810	0.0661
TPP Concentration, X_5	4.1789	0.0500	0.0300	0.0144

Finally, the four selected variables were entered into a multiple linear regression model for the purpose of calculating the overall F-statistics/p-value and an R^2 value to express the overall significance of the model. The resulting equation, equation two with coefficients for mean particle diameter (Y) was as follows:

$$Y = 6821 - 1520X_9 - 1383X_{12} + 2.2X_{10} - 1715X_5 \qquad (2)$$

The ratio of chitosan to TPP, X_9, was identified as the single most important variable ($p=0.001$) in determining mean particle size: the higher the ratio, the smaller the mean particle diameter. This variable explains 31% of the variation in particle size (as indicated by the partial R^2 value of table 4-4). This finding—that the chitosan:TPP ratio plays a role in determining the size of the nanoparticles—is in agreement with the non-statistical

work of Zhang et al,[51] which concluded that particle sizes are dependent upon the chitosan-to-TPP ratios.

The identity of the wash/resuspension solution, X_{12}, was also identified by both selection methods as being significant (p=0.001). The addition of this variable to the model increased the overall R^2 value from 31% to 47% (table 4-4). In other words, the two variables in the model thus far explain 47% of the variations in mean particle diameter, Y. The negative coefficient of this categorical variable indicates that one solution increases the particle size while the other decreases it. In this case, using water resulted in larger particle diameters while PBS produced smaller particles.

The third significant variable selected for the final model was synthesis time, X_{10} (p= 0.0030). As synthesis time increases, particle size also increases. Allowing more time for ionic-gelation synthesis may result in particle-to-particle linking. The last variable of significance selected for the regression model was the TPP concentration, X_5 (p= 0.05). According to the model, increasing the TPP concentration results in smaller particles. Clavo et al.[76] also reported that an increase in TPP concentration produces smaller particles.

Overall, the linear regression model (equation 2) was found to be significant (p=0.001), indicating that the mean particle diameter and the set of selected variables are significantly related. The optimal model containing these four variables accounts for 58% of the observed variation in mean particle diameter. Narrowing down the field of potentially influential preparatory variables from twelve candidates to four significant variables can lead to higher control of determining chitosan particle size.

4.3.2. Morphology and Particle Size Observations

The acidity of the solution used to initially dissolve the chitosan powder exerts a profound influence on particle formation. The use of nanopure water produced particles with no well-defined borders and severe clumping (figure 4-2(a)). With 0.25M acetic acid, we saw nicely formed particles with more defined borders and with very little clumping (Figure 4-2(b)). When the concentration of acid was increased to 0.50M, the particles were slightly formed but were not as well defined as the particles prepared in the 0.25M acid. Moreover, there were signs of chitosan degradation (Figure 4-2(c)). At 0.75M, we saw degradation of chitosan so no particles were formed (Figure 4-2(d)). In summary, using an acetic acid concentration higher than 0.25M seems to impede the proper formation of nanoparticles. Pure water is also unsuitable. Acetic acid with a concentration of 0.25M seems to provide a workable environment for the formation of well-defined spherical particles.

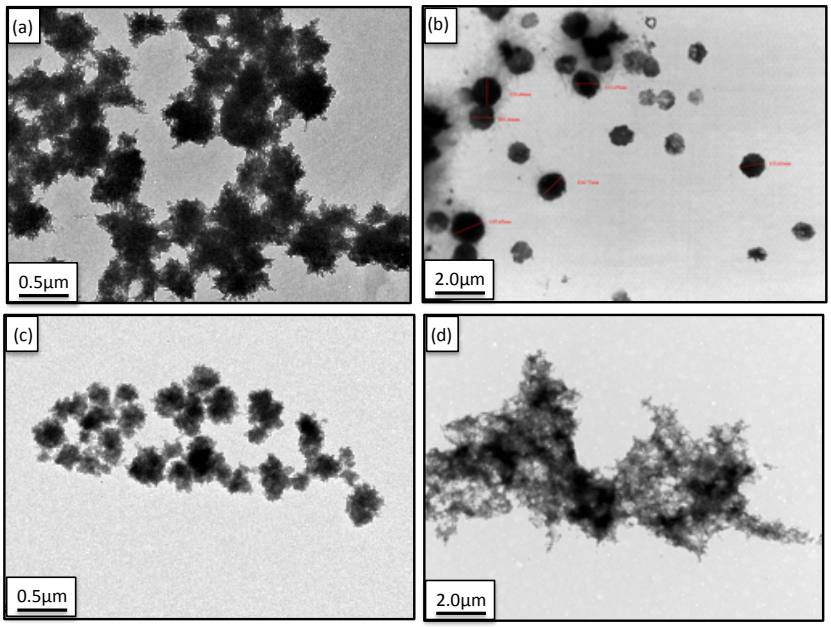

Figure 4-2: TEM images of blank (drug-free) chitosan particles prepared in (a) nanopure water, (b) 0.25M acetic acid solution, (c) 0.50M acetic acid solution, and (d) 0.75M acetic acid solution.

Centrifugation was not statistically selected as being significant in determining mean particle diameter, but quantitative observation using Nanotrac analysis indicated that centrifugation did affect particle size. Figure 4-3 shows the particle size distribution of centrifuged and precipitated samples. Note that the centrifuged sample resulted in predominately microparticles whereas the precipitated sample resulted in mostly nano-sized particles.

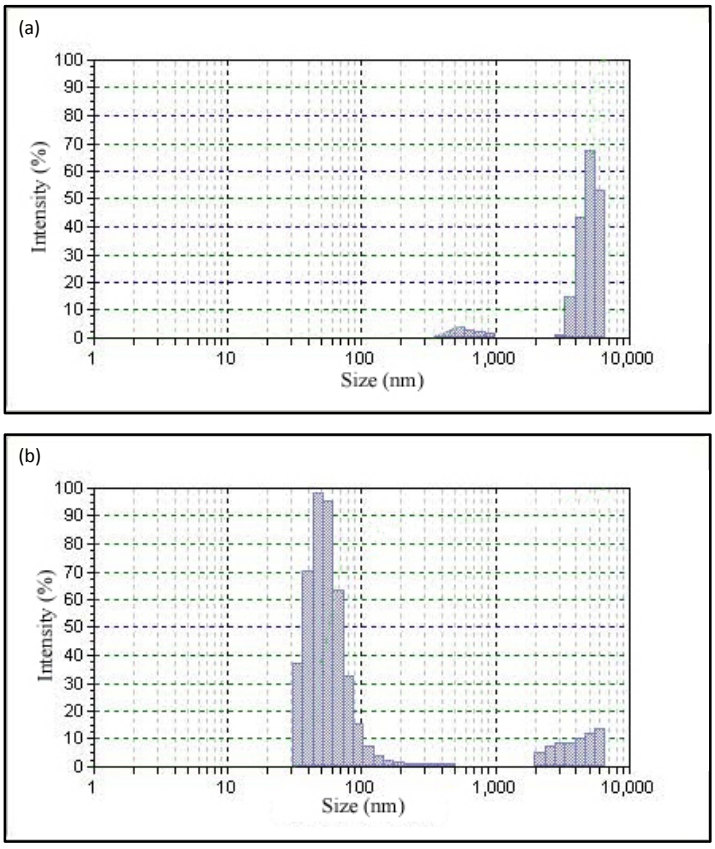

Figure 4-3: Particle size distributions of samples of drug-loaded particles. (a) passively precipitated and (b) centrifuged washed and resuspended in water.

TEM observations corroborated the conclusions drawn from equation 1 regarding the nature of the wash/resuspension solution. When particles were washed with nanopure water, centrifuged, and then resuspended in water, the resulting particle diameters were relatively large due to clumping of smaller particles (Figure 4-4). In contrast, particles washed, centrifuged, and then resuspended in PBS were uniformly spherical and individually distinct, as shown in Figure 4-5.

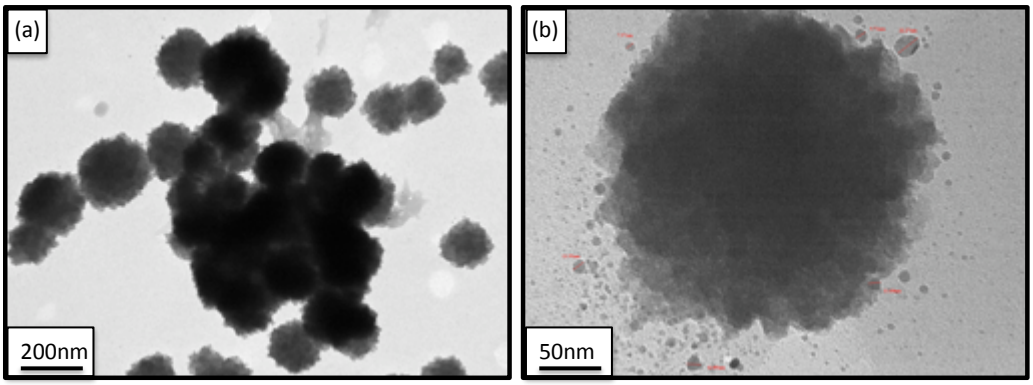

Figure 4-4: TEM images of doxycycline-loaded nanoparticles that were washed, centrifuged, and then resuspended in nanopure water. (a) Several individual particles clumping together, 80kx magnification; (b) an agglomeration of smaller particles, 400kx magnification.

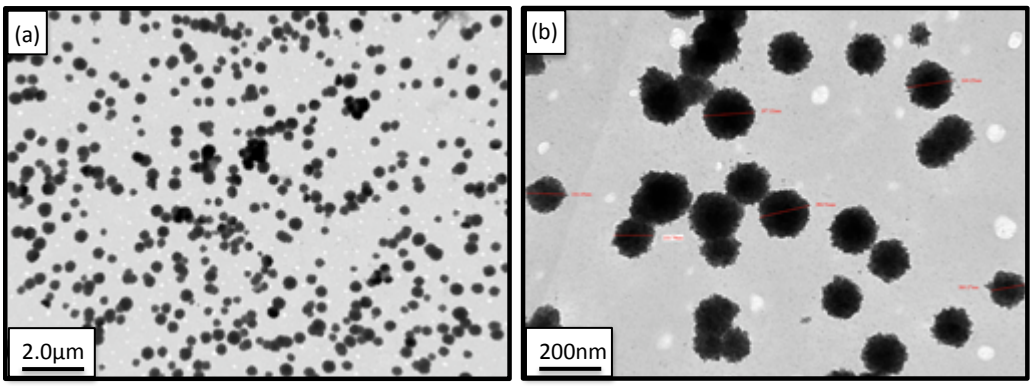

Figure 4-5: TEM images of doxycycline-loaded nanoparticles that were washed, centrifuged, and then resuspended in PBS. Particle diameters range from approximately 160 to 400 nm: (a) 6kx magnification; (b) 60kx magnification.

4.4. Summary

This study showed that chitosan nanoparticles (drug-loaded or drug-free) prepared by the ionic gelation method can be controlled by specific adjustments of the variables involved. The impacts of twelve preparatory variables on particle size were studied using two statistics stepwise forward selection methods. The results of both statistics selection methods showed that the ratio of chitosan to TPP, wash/resuspension solution, synthesis time, and TPP concentration contribute to 58% of the variation in determining the particle size when prepared using the ionic gelation method. All four selected variables were found to be significant ($p=0.001$) in contributing to the particle size. Therefore, this statistical selection of variables can be used to better understand the impact of variables on the particle size, and to improve the preparation of particles using the ionic gelation method.

Chapter 5 - Synergetic Effects of Doxycycline Loaded Chitosan Nanoparticles

This chapter presents the synergetic effects of doxycycline-loaded chitosan nanoparticles. The doxycycline-loaded nanoparticles (DCNPs) were prepared using a modified ionic gelation method with tripolyphosphate (TPP) as a cross-linker. The DCNPs were characterized based on size and size distribution, morphology, drug-release properties, antibacterial activity, and *in vitro* cytotoxicity. Results show that encapsulating doxycycline into chitosan nanoparticles could facilitate intracellular and/or extracellular delivery of the drug and thus improve the drug efficacy in the treatment of bacterial infections.

5.1. Background

In recent years, drug encapsulation and delivery via small particles has garnered increasing interest. Encapsulation may help prevent adverse effects by protecting sensitive tissues from fast drug exposure while also improving drug efficacy by achieving slow, sustained release directly at the infection site. Having patients complete the entire treatment cycle would also increase the likelihood of complete pathogen elimination. These properties suggest that the encapsulation of doxycycline into biodegradable nanoparticles could be used to eventually improve treatment of PID via direct transcervical drug delivery.

A detailed investigation of chitosan nanoparticles as a potential carrier of doxycycline to improve drug delivery and treatment efficacy was performed. Two particle formulations were examined: formulation DCNP6 containing approximately 1.5 times the

crosslinker concentration of the other formulation named DCNP4. As a first step toward assessing this potential, we used an ionic gelation method to synthesize blank and doxycycline-loaded chitosan nanoparticles (DCNPs), which were characterized in terms of several properties relevant to clinical efficacy: particle size, shape, encapsulation efficiency, antibacterial activity, and *in vitro* cytotoxicity.

5.2. Materials and Methods

5.2.1. Materials

Doxycycline, phosphate buffered saline (PBS), Millipore WST-1 Cell Proliferation Assay, and acetic acid were obtained from Fisher Scientific (USA). Sodium tripolyphosphate (TPP), fetal bovine serum, medium 199, and MCDB 105 medium were supplied by Sigma Chemical Company (USA). Partially (75%) deacetylated chitosan (60 kDa) derived from shrimp shells was obtained in powder form from Sigma Aldrich (USA). All other chemicals were of analytical grade and were obtained from a variety of vendors. *Eschericha coli* (ATCC 25922) was purchased from American Type Culture Collection.

5.2.2. Chitosan Nanoparticles Preparation

The chitosan nanoparticles were prepared using the ionic gelation method of Clavo *et al*.[57] Chitosan powder was dissolved, 0.2% weight by volume (w/v), in 0.25M acetic acid; this solution was magnetically stirred overnight at a speed of 400 rpm at room temperature. The acetic acid protonates the amine group of the chitosan molecule, for a more stable interaction with the crosslinking agent and the drug.[59,105] The crosslinker, sodium tripolyphosphate (TPP), was prepared by dissolving the powder in 0.25M acetic acid at two different concentrations: 0.42% w/v (referred here as formulation 8, F8) and

0.60% w/v (formulation 10, F10). In a separate set of experiments, we examined 64 different combinations of solutions and procedural steps, and identified these two formulations as consistently producing particles within a predictable formulation-specific size range.

Blank nanoparticles were formed by combining the chitosan and TPP solutions for a total volume of 2 mL; the chitosan-to-TPP ratio was 23:1 for F8, and 16:1 for F10. To initiate ionic gelation (nanoparticle formation), TPP was added dropwise to the stirred chitosan solution, and the combined solution was then stirred for an additional hour. Blank nanoparticles prepared using F8 (0.42% w/v TPP) are here referred to as BKCNP4 while blanks prepared using F10 (0.60% w/v TPP) are referred to as BKCNP6. The solution with precipitated nanoparticles was centrifuged at 10,000 rpm for 5 minutes, and the resulting supernatant was saved for later analysis of its doxycycline content. The particles in the microcentrifuge tube were washed/resuspended by adding 2 mL nanopure water, and the tube was again centrifuged at 10,000 rpm for 5 minutes. The second supernatant was removed and discarded as preliminary tests had shown that the second supernatant contained no doxycycline residue. Finally, the particles were resuspended in 2mL nanopure water before further analysis.

A doxycycline stock solution was prepared by dissolving doxycycline powder in nanopure water to achieve a final concentration of 200 mg doxycycline per mL solution. Drug-loaded chitosan nanoparticles were then prepared according to the procedure outlined above, except that 100 µL of the doxycycline stock solution was added dropwise to the stirred chitosan solution just before the TPP addition. In every batch of DCNP solution, the final doxycycline concentration was 20 mg/mL. Drug-loaded chitosan nanoparticles prepared using 0.42% w/v TPP are here referred to as DCNP4; those prepared with 0.60% w/v TPP are referred to as DCNP6. All analyses of blank particles,

drug-loaded particles, and supernatant were initiated within 24 hours of particle preparation.

5.2.3. Nanoparticles Characterization

Particle size distributions for blank nanoparticles and DCNPs were determined with a Microtrac Particle Size Analyzer, which measures dynamic light scattering by particles in solution. The analyses were performed on samples of nanoparticles suspended in 1 mL of nanopure water. The shapes of the blank particles and DCNPs were examined using a JEOL 1400 transmission electron microscope (TEM) with a 0.38 nm assurance for point to point images and 0.2 nm for lattice images. Particles to be used for TEM examination were first dried under vacuum and stored in the dark at 4°C. TEM samples were then prepared by depositing a drop of nanoparticles onto a formvar-coated copper grid, which was allowed to dry by vacuum before TEM analysis.

5.2.4. Encapsulation Efficiency

Incorporation of doxycycline into the particles was characterized by measuring the doxycycline contained in the centrifugation supernatant. Since the total amount of drug in each formulation batch was known (2 mL solution with a doxycycline concentration of 20 mg/mL), any doxycycline not found in the supernatant could be assigned to the particles. Doxycycline in the supernatant was quantified using a Nano-drop spectrophotometer (ND-1000), which has an absorbance precision of 0.003 at 1 mm (0.01 cm) path length. According to the Beer-Lambert Equation, the doxycycline concentration, c, is given by $c=A/\varepsilon L$, where A is light absorbance at 220 nm wavelength, ε is the molar absorptivity coefficient (121.39 M^{-1} cm^{-1}), and L is the path length (0.01

cm). All measurements were performed in triplicate (*n=3*). The encapsulation efficiency (*EE*, %) was calculated using equation 3:

$$\text{EE (\%)} = \frac{\text{Drug Used @ Synthesis (mg/mL)} - \text{Free Drug in Supernatant (mg/mL)}}{\text{Drug Used @Synthesis (mg/mL)}} \times 100 \qquad (3)$$

5.2.5. Assessment of Drug Release

To determine the rate at which doxycycline was released by the nanoparticles, the particles were resuspended in a drug-free solution that was analyzed for doxycycline content at predetermined time interval. To begin, dried fresh nanoparticles of known antibiotic content were first resuspended in 2 mL of nanopure water. A small aliquot of this particle-laden solution was then added to PBS-ethanol solution to produce a final volume of 2 mL with an initial concentration of 100-µg doxycycline per mL. This solution was incubated at 37°C under gentle agitation. At each specified time point (0.5, 1, 2, 3, 4, 5, 6, 7, 8, 16, and 24 hours) thereafter, the sample was centrifuged and the supernatant was isolated and analyzed by Nano-drop spectrophotometry to determine the amount of doxycycline in solution. All measurements were performed in triplicate (*n*=3) for each formulation. The percentage of drug released at each time point was calculated according to equation 4:

$$\text{Drug Release (\%)} = \frac{\text{Drug in Solution (µg/mL)}}{\text{Initial Drug in Particles (µg/mL)}} \times 100 \qquad (4)$$

5.2.6. Antimicrobial Activity Assessment

To determine the antibacterial activity of the doxycycline-loaded chitosan nanoparticles, minimum inhibitory concentrations (MICs) and minimum bactericidal concentrations (MBCs) were evaluated. The procedures for both assays were adopted from Lee et al.[106] MIC is the lowest concentration of DCNPs that inhibits bacterial

growth. For our analyses, a visual turbidimetric method was used. Freshly prepared nanoparticles, blank and drug-loaded, were UV-sterilized for ten minutes. The particles were then resuspended in a volume of sterile water sufficient to achieve a final doxycycline concentration of 100 µg/mL. A 500 µL aliquot of this solution with sterilized particles was added to a tube containing Luria-Bertani (LB) broth for a total volume of 2 mL. A serial dilution, with a dilution factor of 0.3, was performed for the remaining six tubes. A parallel series of experiments was also run using unencapsulated doxycycline.

Under sterile conditions, the tubes containing particles were inoculated with 1.0×10^5 colony-forming units (CFUs)/mL of *Escherichia coli* cells in LB broth, then incubated at 37°C under agitation for four hours. Following the incubation, the tubes were assessed visually for the appearance of turbidity (i.e., bacterial growth). Among the tubes that showed no visual turbidity—that is, complete inhibition of visible *E. coli* growth—the one with the lowest doxycycline concentration was identified as the MIC tube for that series. All MIC tubes were analyzed to assess the amount of bacteria present by measuring optical density of the suspension at 600 nm (OD_{600}) and then calculating the number of bacterial cells present.

The MBC is the minimum concentration of DCNPs that will kill 99% of the bacterial cells initially present. To determine this value, 100 µL aliquots of liquid culture (broth + nanoparticles + bacteria) from each series' MIC tube and the two tubes prior (i.e., containing slightly more doxycycline) were plated and incubated at 37°C overnight. As a positive control, an additional plate was plated with broth plus *E. coli* (no particles or drug); as a negative control, another plate was plated with broth plus blank particles plus *E. coli* (no drug). All samples were plated in triplicate. Plates were observed for colony growth, and the plate with the fewest colony colonies was identified as the MBC plate.

5.2.7. Cytotoxicity Assessment

Cytotoxicity of the DCNPs was determined by treating normal human ovarian surface epithelial (OSE) cells with different concentrations of doxycycline-loaded nanoparticles, then monitoring cell viability over the next five days. The OSE cells were cultured for 4 to 7 days in flasks containing medium199/MCDB105 media supplemented with 10% fetal bovine serum. The cells were removed from the flasks and counted, and then 100 µL of medium containing cells was added to the wells of a 96-well plate to give final cell concentrations of 5×10^2, 1.0×10^3, or 2.0×10^3cells/mL. After 24 hours incubation at 37°C, the cells were treated with blank nanoparticles, DCNP4 (1 and 2 µg/mL), DCNP6 (1 and 2 µg/mL), or unencapsulated doxycycline (1 and 2 µg/mL). The plate was then incubated at 37°C. Bright microscopy was used to examine the cell morphology after treatment just before the assessing for cytotoxicity. Cytotoxicity was assessed on days 1, 3, and 5 by WST-1 assay. WST-1 assay reagent (10 µL) was added to each well, followed by incubation for another 4 hours at 37°C and then spectrophotometric assessment of cell viability.Mitochondrial dehydrogenases produced by viable cells reduce the WST-1 reagent to form formazan dye in an amount directly proportional to the number of metabolically active cells in the well. This dye was quantified using a Biotex Synergy multiplate reader to measure absorbance at 450 nm (reference wavelength was 630 nm). All treatments were assayed in triplicate (*n*=3) and calculated according to equation 5:

$$\text{Cell Viability (\%)} = \frac{\text{OD}_{450} \text{ of Treated Cells}}{\text{OD}_{450} \text{ of Treated Cells}} \times 100 \qquad (5)$$

5.2.8. Statistical Analysis

A two-way analysis of variance (ANOVA) was employed to identify statistical differences among the various experimental groups and their corresponding control groups. Experimental groups with p-values of $p<0.05$ were considered to be statistically significant.

5.3. Results and Discussion

5.3.1. Characterization of Doxycycline Loaded Nanoparticles

Blank and doxycycline-loaded chitosan nanoparticles were successfully prepared using an ionic gelation method. The blank particles, BKCNP4 and BKCNP6, were relatively large, with an average diameter of 4,900 nm and 4,450 nm, respectively (data not shown). Both groups of particles were spherical in shape with a narrow particle size distribution. The drug-loaded particles were smaller than their blank counterparts. The DCNP4 particles (Figure 5-1(a)), with an average particle diameter of 44.50 nm, were two orders of magnitude smaller than their corresponding blanks and had a wider particle size distribution profile. DCNP4s were spherical in shape with smooth edges (Figure 5-1(b)). Similarly, the DCNP6 particles (Figure 5-1(c)), with an average diameter of 280 nm, were small compared to their blank counterparts—about 1/15 the size--but were significantly larger than the DCNP4s. In contrast to the DCNP4s, the DCNP6 particles exhibited a very narrow particle size distribution profile. The DCNP6 particles were spherical like the DCNP4s but had edges that were not as smooth (Figure 5-1(d)).

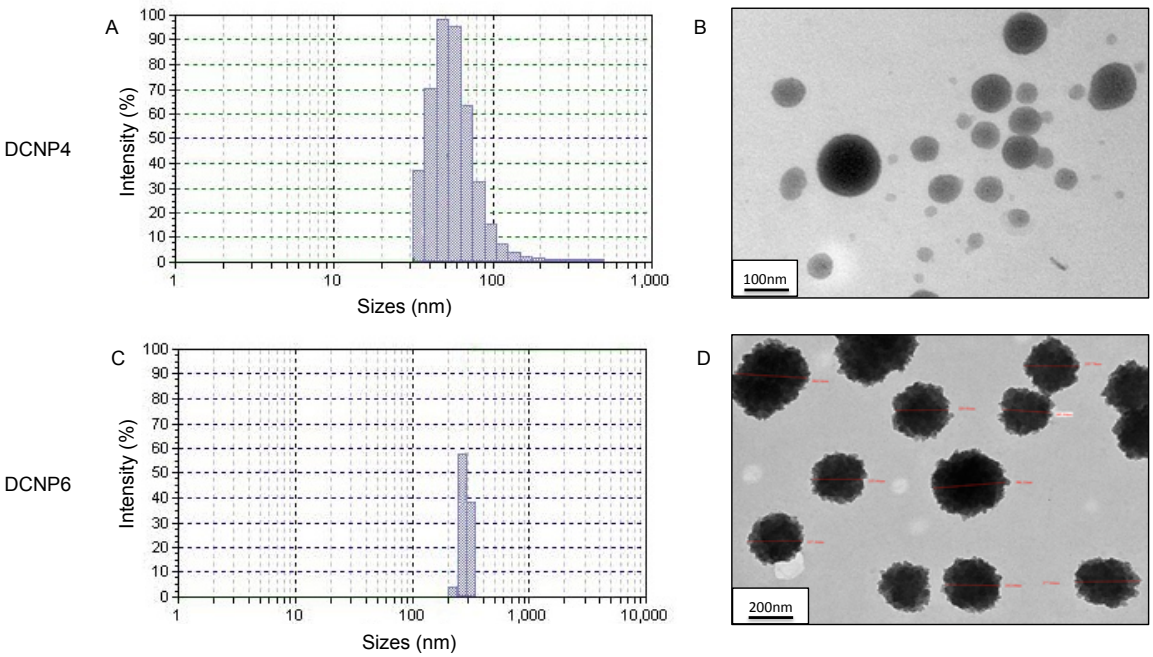

Figure 5-1: Particle size distribution and TEM images for DCNP4 (top) and DCNP6 (bottom).

Since the conditions that varied between the two formulations for preparing these particles was the concentration of the TPP crosslinker and the resulting ratio of chitosan to TPP, based on the data from the previous chapter, we now know that the concentration of the crosslinker plays a role in determining particle size. Also, inclusion of the doxycycline in the formulations produced particles significantly smaller than the blanks, which is an interesting finding that our group is currently investigating. Having a narrower particle size distribution profile—i.e., particles of more uniform size--is also important. The more similar the particles are in size, the more equally the drug will be distributed among the particles, which will normalize the rate of drug release.

5.3.2. Encapsulation Efficiency

Across all batches of DCNP4, the lowest encapsulation efficiency was 22%, the highest was 69%, and the average was 53%±19. For DCNP6, the lowest encapsulation efficiency was 41%, the highest was 68%, and the average was 56%±10. Even though DCNP6 was substantially larger in diameter, there was no significant difference in the amount of drug encapsulated for each type of DCNP.

5.3.3. Drug Release

Doxycycline was released from the DCNPs in a burst-effect manner followed by a slow sustained release (Figure 5-2). For DCNP4, the burst effect occurred within the first five hours; for DCNP6, within the first four hours. Within the first couple of hours after this initial burst, the amount of drug released decreased, then, it was followed by a sustained release for the remaining time. By the end of the 24-hour monitoring period, DCNP6 had released more total drug than the DCNP4. The difference between the amounts of drug released by the two different particle formulations can be attributed to the differences in particle size, with the larger particles (DCNP6) releasing more antibiotic than the smaller ones (DCNP4). A burst effect followed by slow sustained release, as demonstrated by both nanoparticle formulations, is ideal for treating microbial infections such as PID. For PID, delivering the particles in a local (i.e., transcervical) manner to the reproductive lumen would provide an increasing amount of doxycycline in the beginning, followed by a reduced amount afterwards. This would increase the likelihood of total pathogen elimination.

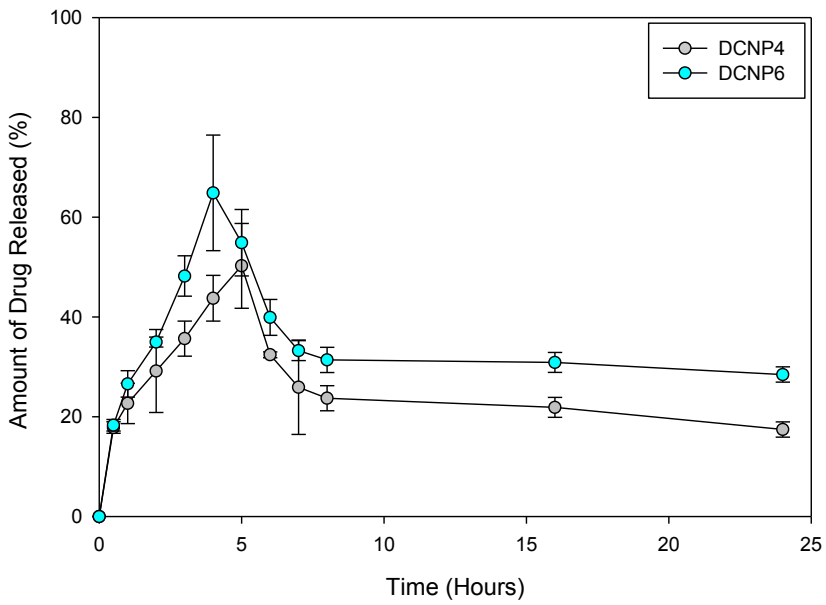

Figure 5-2: The amount of doxycycline release over a 24-hour period for DCNP4 and DCNP6. Both had an initial burst effect within the first four to five hours. Then, there was a decrease in the amount of drug being released followed by a slow sustained amount for the remaining hours. Data shown are the mean ± standard deviation (n=3).

5.3.4. Antimicrobial Activity Assessment

After four hours incubation at 37°C, the drug-loaded nanoparticles' minimum inhibitory doxycycline concentration, MIC, was 16 µg/mL for DCNP4 and 13 µg/mL for DCNP6. Figure 5-3 shows the MIC cases for DCNP4 (16 µg/mL) and DCNP6 (13 µg/mL) with unencapsulated doxycycline (Doxy-13µg/mL) and blank particles serving as controls. For both types of DCNPs, more than 92% *E. coli* growth inhibition was observed. The minimum bactericidal concentration, MBC, was 48 µg/mL and 40 µg/mL for DCNP4 and DCNP6, respectively. Unencapsulated doxycycline treatments (Doxy), conducted at the same concentrations as the DCNP drug concentrations, resulted in the near-elimination of *E. coli*. These data suggest that the unencapsulated doxycycline had a higher antibacterial activity than the DCNPs within the four-hour period. However,

because the DCNPs release the doxycycline in a slow and sustained manner, we speculate that the nanoparticles' antibacterial activity would have been higher if the incubation period had been extended beyond four hours.

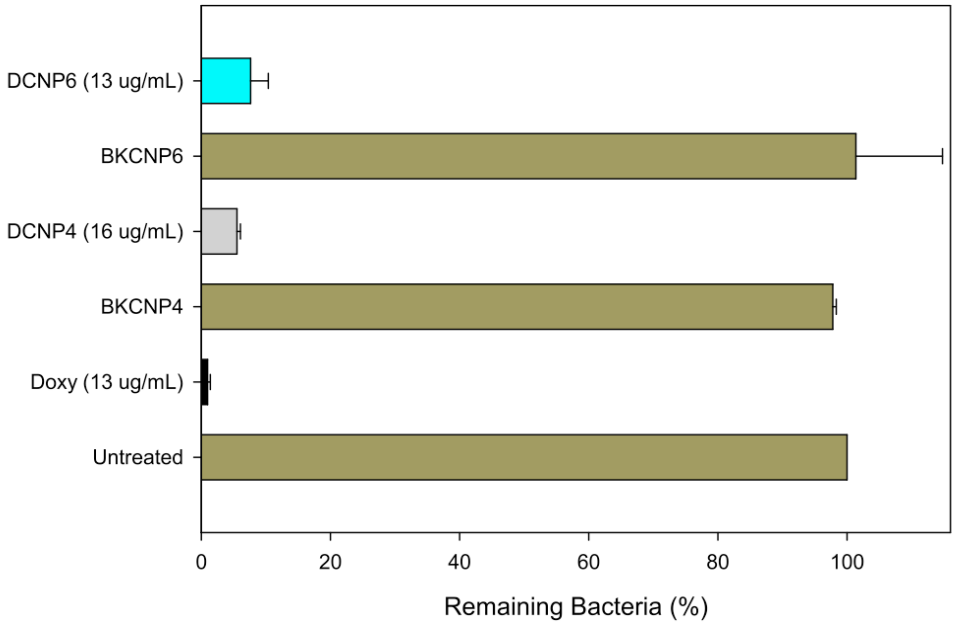

Figure 5-3: Inhibitory effects of drug-loaded chitosan nanoparticles on bacterial growth, expressed in terms of percentage of remaining bacteria after four hours of treatment. MIC values are as follow: DCNP4 = 16 μg/mL, DCNP6 = 13 μg/mL, and Doxy = 13 μg/mL. The untreated tube was used to define the "100% remaining" (no inhibition) case. Data shown are the mean ± standard deviation (n=3).

5.3.5. Cytotoxicity Assessment

For the case of initial human ovarian surface epithelial (OSE) cell densities of 5×10^2, no cytotoxicity (relative to the cells-only case) was induced by the 1 μg/mL or 2 μg/mL dosages of either DCNP formulation. In other words, cells treated with the DCNPs for five days showed high cell viability (Figure 5-4). In fact, a significant increase in cell proliferation relative to the cells-only case was often observed when the OSE cells were treated with blank or doxycycline-loaded nanoparticles. In contrast, unencapsulated doxycycline at the same dosages induced severe cell toxicity: only 39% of the original

population remained viable after the five-day treatment. Cells treated with both dosages of DCNP4 or with BKCNP4 had a higher viability than the untreated cells. For DCNP6, the viability of cells treated with 1 μg/mL was higher than for untreated cells, but cells treated with 2 μg/mL showed lower viability. Nevertheless, the DCNP6 case still showed greater cell viability than the unencapsulated drug treatments. Data from the wells with 1.0×10^3 and 2.0×10^3 initial cell densities are not presented because of cell overcrowding over the five-day period.

DCNP4

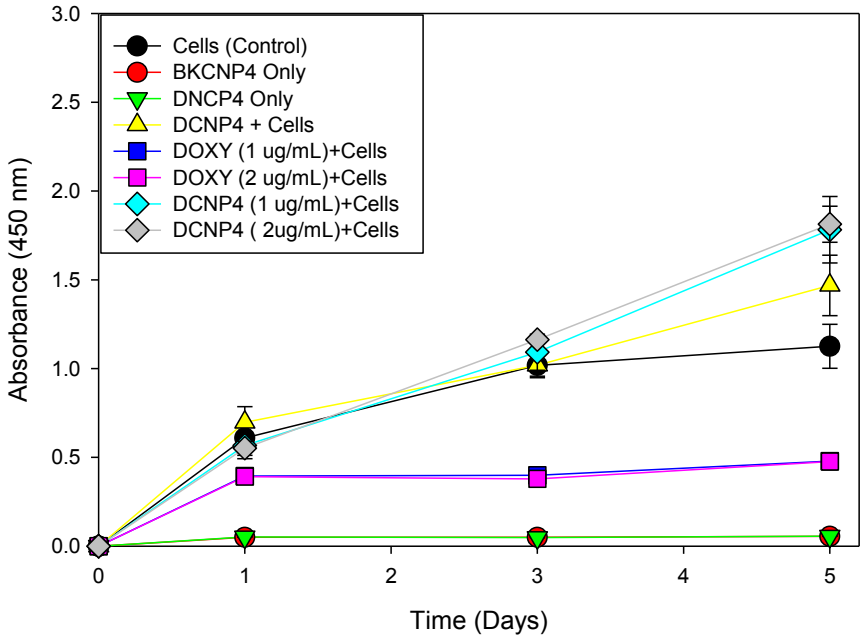

DCNP6

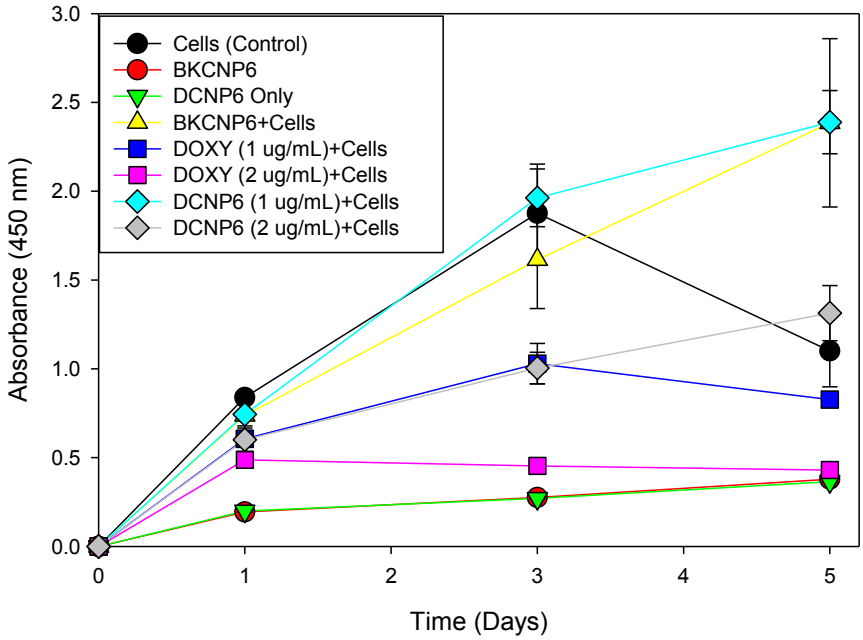

Figure 5-4: Five-day cell viability for human ovarian surface epithelial cells exposed to blank nanoparticles, drug-loaded nanoparticles, and unencapsulated doxycycline. A higher formazan absorbance indicates greater cell viability. Data shown are the mean ± standard deviation (n=3).

These cytotoxicity results show that encapsulation of doxycycline into the chitosan polymer reduces the toxicity that is normally induced by the unencapsulated drug. The differences between the DCNP4 and DCNP6 cytotoxicity results are possibly due to the differences in their size and the amount of drug released. The DCNP6s were observed to release more doxycycline than the DCNP4s. Further exploration and evaluation of the effects of chitosan particles on cell growth is necessary to explain the observed increase in proliferation.

Doxycycline-induced cytotoxicity was confirmed visually through observations of cell morphology following exposure to doxycycline. Cells treated with 1 μg/mL and 2 μg/mL dosages of doxycycline show the morphology of dead cells. The morphological effects of treating with DCNP4 (at 2 μg/mL) and unencapsulated doxycycline (also at 2 μg/mL) are illustrated in Figure 5-5. Note that the cells treated with the DCNPs were of the same morphology as the untreated cells. This further demonstrates that encapsulation of doxycycline into chitosan nanoparticles minimizes the adverse effects of the drug.

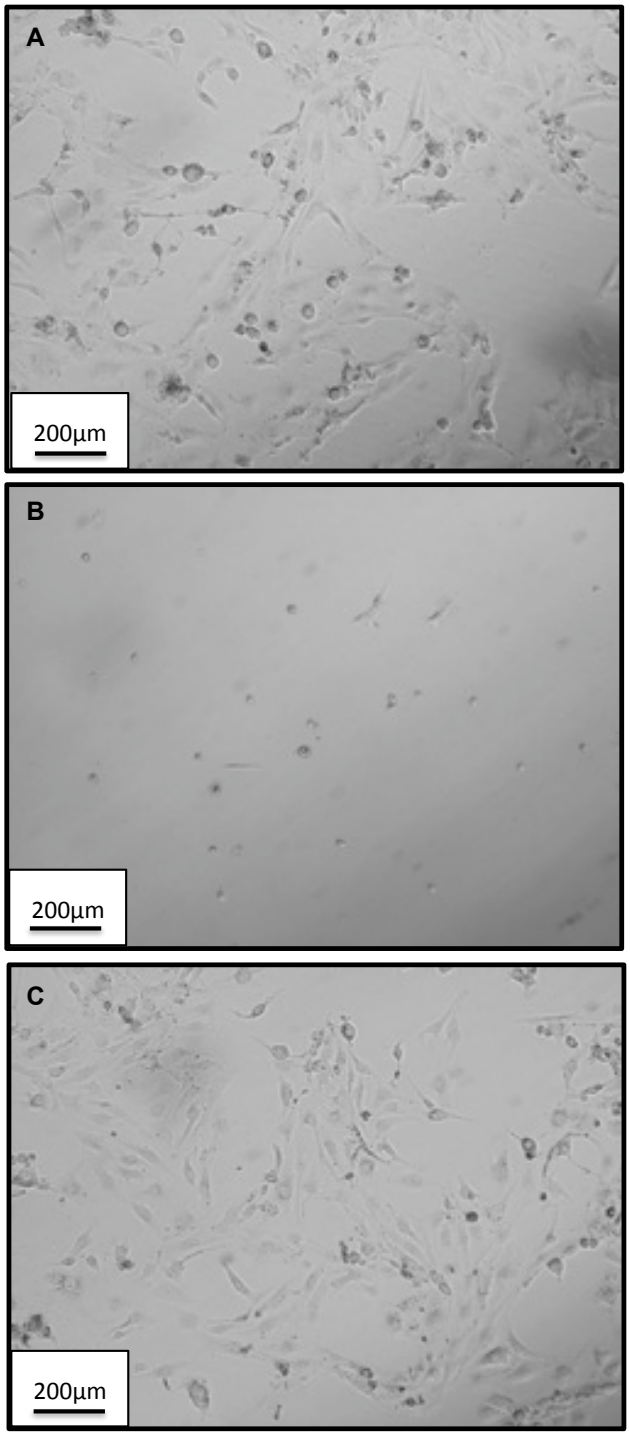

Figure 5-5: Bright-field images of human ovarian surface epithelial cells after being exposed to the different treatments. (a) No treatment (control), (b) doxycycline at 2 µg/mL, and (c) DCNP4 at 2 µg/mL. Magnification 10X.

5.4. Summary

Doxycycline-loaded chitosan nanoparticles were synthesized and characterized to analyze their properties for targeted drug delivery. Two types of nanoparticles were formulated with differing concentrations of crosslinker: DCNP4 and DCNP6. The DCNP6 formulation contained approximately 1.5 times more TPP crosslinker than DCNP4. Results showed that both types of drug-loaded chitosan nanoparticles were spherical, with encapsulation efficiencies of approximately 50%, and with a similar drug release profile. Both formulations also inhibited the growth of *Escherichia coli* after four hours of incubation. MBC (minimum bactericidal concentration) values were less than 50 μg/mL. The DCNPs induced significantly less apparent cytotoxicity than the unencapsulated doxycycline. These results demonstrate that the encapsulation of doxycycline into chitosan nanoparticles has the potential to minimize adverse drug side effects.

Chapter 6 - Summary, Conclusions, and Future Work

This chapter provides a summary of the research work and findings of the dissertation. The conclusions are discussed here followed by a description of future research work.

6.1. Summary

This dissertation focused on the design and validation of a new device and approach to collect sterile specimen samples from the endometrium for more accurate PID diagnosis, and to locally treat PID using doxycycline-loaded chitosan nanoparticles. In the first part of this dissertation, we designed and developed a sterile uterine sampler device for uncontaminated endometrium sampling. Then, we analyzed the ionic gelation method for preparing the doxycycline-loaded chitosan nanoparticles and identified relationships between the variables and particle size. Finally, we studied the *in vitro* antibacterial and cytotoxicity effects of the doxycycline-loaded chitosan nanoparticles.

A novel single use sterile uterine sampler cover (SUSC) device was designed and developed that has two main functions: to safely and effectively collect uncontaminated specimen samples from the uterus, and to deliver nano-encapsulated drugs directly to the site of infection. The developed device was designed to accommodate any size of cervices and collect up adequate specimen sample. The device was validated using an agar sampling test that demonstrated the capability of the presented SUSC device to significantly reduce contamination of the collected sample.

In the second part of the dissertation, we analyzed twelve preparatory variables relevant in determining chitosan particle sizes by the ionic gelation method. Statistical analysis was performed to select significant variables that were used to build an optimal model for determining the particle size. The statistical study showed that the mean particle diameter of chitosan particles (drug-free or drug-loaded) prepared by the ionic gelation method can be manipulated by varying four key formulation parameters. Based on two independent statistical methods, these parameters are: the chitosan-to-TPP ratio, wash/resuspension solution, synthesis time, and TPP concentration. These four variables contributed to 58% of the total variation in observed particle size. Mean particle diameter was found to be directly proportional to synthesis time and inversely proportional to the chitosan-to-TPP ratio and TPP concentration. In other words, increasing the chitosan-to-TPP ratio, and TPP concentration while lowering the synthesis time can lead to the formation of smaller particles. Using PBS as the wash/resuspension solution instead of water also decreases the particle size. In addition, it was observed that dissolving or protonating chitosan in acetic acid of concentration higher than 0.25M resulted in chitosan degradation. From the TEM studies, it was observed that centrifugation (rather than passive settling) of the particles followed by resuspension in nanopure water (rather than PBS) result in severe particle clumping (aggregate) and larger particle diameters.

In the third part of the dissertation, two particle formulations were examined in more detail: formulation DCNP6 containing approximately 1.5 times the crosslinker concentration of the other formulation named DCNP4. Both formulations produced spherically shaped drug-loaded nanoparticles. The spheres ranged in size from 30 to 220 nm diameter for DCNP4 and 200 to 320 nm diameter for DCNP6. Average encapsulation yield was 53% for DCNP4 and 56% for DCNP6. In terms of drug release, both formulations showed a burst effect within the first four to five hours, followed by a

slow sustained release for the remainder of the 24-hour monitoring period. The *in vitro* antibacterial activity against *Escherichia coli* was high, with both formulations achieving more than 90% inhibition of four-hour bacterial growth. Cytotoxic effects of the DCNPs on normal human ovarian surface epithelial cells were significantly lower than those of unencapsulated doxycycline. After five days, cultures exposed to the unencapsulated antibiotic showed a 61% decrease in cell viability, while cultures exposed to the DCNPs exhibited less than a 10% decrease.

6.2. Conclusions

This dissertation presented a new device and nanoparticle-based approach to improve the accuracy of diagnosis and treatment of pelvic inflammatory disease (PID). A new device was developed to procure sterile specimen samples from the endometrium by passing through highly contaminated vaginal and distal cervical areas. It is expected that the analysis of uncontaminated endometrium tissue samples will provide accurate diagnosis of PID, the specific organism causing it, and the particular drug to be administered. The presented device can also be used for directly delivering nanoencapsulated drugs at the site of infection. We analyzed the encapsulation of doxycycline into chitosan nanoparticles using the ionic gelation method to better understand the size variation of the particles produced through this method. Four preparatory variables were selected as being significantly influential in determining particle size. Eventually, this work can lead to higher control of particle size and morphology (shape), which may in turn facilitate the use of the ionic gelation method for mass production of chitosan particles for drug delivery systems. Finally, we demonstrated that doxycycline-loaded chitosan nanoparticles have the potential for treating *E. coli,* a common co-pathogen in pelvic inflammatory disease, in a slow

sustained manner without inducing any apparent cellular toxicity to the non-bacterial cells. These laboratory results suggest that doxycycline-loaded chitosan nanoparticles show promise for use in transcervical drug delivery and improved efficacy in the treatment of bacterial uterine infections. These results also demonstrate that the encapsulation of doxycycline into chitosan nanoparticles can minimize the adverse side effects of the drug while also beneficially releasing the drug in a slow and sustained manner.

The findings of this dissertation research are not only beneficial for the diagnostic of PID but also for localized delivery of nanoencapsulated drugs to the uterus. Uncontaminated samples will allow a better understanding of the natural microbial ecology of the uterus under a variety of spontaneous and manipulated hormonal conditions. It is highly likely that microfilms of dormant pathogens exist in the endometrial cavity as they do in the inner ear, bladder and prostate, and this has enormous implications for fertility and complications of pregnancy. The SUSC device can also be used for addressing other gynecological disorders/problems such as removal of obstructions in the fallopian tubes, and targeted sperm delivery.

6.3. Future Work

Based on the findings of this dissertation, the following future studies are recommended.

6.3.1. SUSC Device Clinical Testing

Once the patent process of the device is completed, the SUSC device will be manufactured so that it can be eventually approved for clinical testing. First, the proper

IRA will be filed and upon approval from the IRA office, patients undergoing hysterectomy will be asked to consider being a volunteer in our clinical testing.

6.3.2. Cellular Growth Induced by Chitosan Particles

From the cytotoxicity work, we found that the blank nanoparticles induce cellular growth. Future work will consist of studying whether the blank and drug-loaded particles used in this study induce cell proliferation in other cell types. Contingent upon the result of those preliminary studies, chitosan could be studied for its potential role in wound healing.

6.3.3. The Effect of DCNPs on Intracellular Organisms

Based on the results from this dissertation, we demonstrated that the chitosan nanoparticles are entering the cells. We also know that the DCNPs are inhibiting the growth of *E. coli.* The next step is to evaluate the effects of the DCNPs on intracellular infectious organisms such as *Neisseria gonorrhoeae* and *Chlamydia trachomatis,* which contribute to two of the most common sexual transfected diseases. In order to treat infections that are caused by intracellular organisms, the drug needs to be delivered into the cells/tissues. The nanoparticle delivery system presented in this dissertation would be ideal for treating these types of infections.

6.3.4. Biofilm Studies

In this dissertation, we analyzed the effect of the doxycycline-loaded chitosan nanoparticles against *E.coli* in planktonic conditions. Based on the results from chapter 5, the next step would be to analyze the effect of the doxycycline-loaded chitosan nanoparticles in a biofilm system, preferably a biofilm model that is similar to that of the

uterus biofilm. Results from inhibitory tests done in a biofilm system will improve the clinical value for future application of these doxycycline-loaded chitosan nanoparticles in drug delivery.

6.3.5. Animal Studies

After studying the doxycycline-loaded chitosan in a biofilm model, these particles can then be evaluated *in vivo*. We know from the in vitro studies that the chitosan nanoparticles do not induce any form of cytotoxicity. However, it is important to know how these nanoparticles will function in an animal model. At this phase of the study, the particles should be delivered in a transcervical manner with a miniature version of the SUSC device. An ideal animal model would be one that has an infection in the uterus similar to PID on humans.

References

1. Crossman S. The Challenge of Pevic Inflammatory Disease. *American Family Physician.* 2006;73(5):859-864.

2. Haggerty C, Ness R. Newest Approaches to Treatment of Pelvic Inflammatory Disease: A Review of Recent Randomized Clinical Trials. *Clinical Infectious Diseases.* 2007;44:953-960.

3. Walker C, Wiesenfeld H. Antibiotic Therapy for Acute Pelvic Inflammatory Disease: The 2006 Centers for Disease Control and Prevention Sexually Transmitted Diseases Treatment Guidelines. *Clinical Infectious Diseases.* 2007;44(S111-22).

4. Sweet R. Role of Bacterial Vaginosis in Pelvic Inflammatory Disease. *Clinical Infectious Diseases.* 1995;20(2):271-275.

5. Peterson HB, Galaid EI, Zenilman JM. Pelvic Inflammatory Disease: Review of Treatment Options. *Reviews of Infectious Diseases.* 1990;12(6):656-664.

6. Rein DB, Kassler WJ, Irwin KL, Rabiee L. Direct Cost of Pelvic Inflammatory Disease and Its Sequelae: Decreasing but Still Substantial *Obstetrics and Gynecology.* 2000;95(3):397-402.

7. Bell JD, Bergin IL, Schmidt K, Zochowski MK, Aronoff DM, Patton DL. Nonhuman Primate Models Used to Study Pelvic Inflammatory Disease Caused by Chlamydia trachomatis. *Infect Dis Obstet Gynecol.* 2011:1-7.

8. Soper DE. Pelvic inflammatory disease. *Obstet Gynecol.* 2010;116(2):419-428.

9. Centers for Disease Control and Prevention (CDC). Cephalosporin susceptibility among Neisseria gonorrhoeae isolates--United States, 2000-2010. *MMWR Morb Mortal Wkly Rep.* 2011;60(26):873-877.

10. Beigi R, Wiesenfeld H. Pelvic Inflammatory disease: new diagnostic criteria and treatment. *Obstetrics and Gynecology Clinics of North America.* 2003;30:777-793.

11. Hay PE, Pittrof R. Has the effectiveness of a single chlamydia test in preventing pelvic inflammatory disease over 12 months been overestimated? *Women's Health.* 2010;6(5):627-630.

12. Dayan L. Pelvic Inflammatory Disease. *American Family Physician.* 2006;36(11):858-862.

13. Jaiyeoba O, Soper DE. A Practical Approach to the Diagnosis of Pelvic Inflammatory Diseas. *Infect Dis Obstet Gynecol.* 2011:1-6.

14. Wiesenfeld HC, Hillier SL, Krohn MA, et al. Lower Genital Tract Infection and Endometritis: Insight Into Subclinical Pelvic Inflammatory Disease. *The American College of Obstetricians and Gynecologists.* 2002;100(3):456-463.

15. Centers for Disease Control and Prevention. Sexually Transmitted Diseases Treatment Guidelines. *MMWR.* 2010;59(No. RR-12):1-109.

16. Moore DE, Spadoni LR, Foy HM. Incresed frequency of serum antibodies to Chlamydia trachomatis in infertility due to distal tubal disease. *Comparative Study* 1982;2(8298):547-547.

17. Punnonen R, Terho P NV, Meurman O. Chlamydial serology in infertile woman by immunofluorescence. *Fertil Steril.* 1979;31(6):656-659.

18. Wolner-Hanssen P. Silent pelvic inflammatory disease: is it overstated? *Obstet Gynecol.* 1995;86(3):321-325.

19. Shepard MK, Jones RB. Recovery of Chlamydia trachomatis from endometrial and fallopian tube biopsies in women with infertility of tubal origin. *Fertil Steril.* 1989;52(2):232.

20. Keilani A, Boulieu D, Raudrant D, Carraz M, Quenin P. Role of Chlamydia trachomatis in tubal pathology (acute salpingitis and tubal sterility). Microbiological study of 175 samples of peritoneal fluid. *J Gynecol Obstet Biol Reprod (Paris).* 1989;18(2):167-172.

21. Ross JD. An Update on Pelvic Inflammatory Disease. *Sex Transm Inf.* 2002;78:18-19.

22. Peipert J, Boardman L, Hogan J, Sung J, Mayer K. Labortory Evaluation of Acute Upper Genital Tract Infection. *Obstetrics and Gynecology* 1996;87:730-736.

23. Henry-Suchet J. PID: Clinical and Laparoscopic Aspects. *Ann N Y Acad Sci.* 2000;900:301-308.

24. Goshen T, Shpigel NY. Evaluation of intrauterine antibiotic treatment of clinical metritis and retained fetal membranes in dairy cows. *Theriogenology.* 2006;66(9):2210-2218.

25. Stubbs E, Schamp A. The evidence is in. Why are IUDs still out? Family physicians' perceptions of risk and indications. *Can Fam Physician.* 2008;54(4):560-566.

26. Heinberg EM, McCoy TW, Pasic R. The Perforated Intrauterine Device: Endoscopic Retrieval. *JSLS.* 2008;12(1):97-100.

27. The ESHRE Capri Workshop Group. Intrauterine devices and intrauterine systems. *Human Reproduction Update.* 2008;14(3):197-200.

28. Humber N. The occasional D & C. *Can J Rural Med.* 2009;14(3):115-118.

29. Chambers JT, Chambers SK. Endometrial Sampling: When? Where? Why? With What? *Clinical Obstetrics and Gynecology.* 1992;35(1):28-39.

30. Cooper JM, Erickson ML. Endmetrial Sampling Techniques in the Diagnosis of Abnormal Uterine Bleeding. *Obstetrics and Gynecology Clinics of North America.* 2000;27(2):235-244.

31. Guilbeau JA, Schaub IG. Uterine Cutlture Technique: A simple Method for Avoiding Contamination by the Cervical and Vaginal Flora. *American Journal of Obstetrics & Gynecology.* 1949:407-410.

32. Knuppel R, Scerbo J, Dzink J, Mitchell G, Cetrulo C, Barlett J. Quantitive Transcervical Uterine Cultures With a New Device. *Obstetrics and Gynecology.* 1981;57:243-247.

33. Duff P, Gibbs R, Blanco J, St. Clair P. Endometrial Culture Techniques in Puerperal Patients. *Obstetrics and Gynecology.* 1983;61(2):217-222.

34. Bollinger CC. Bacterial Flora of the Nonpregnat Uterus: A New Culture Technic. *Obstetrics and Gynecology.* 1964;23(2):251-255.

35. Binard W.J., Dye J.F., Inventors; The Kendall Company, assignee. Endometrial Sampler 1973.

36. Shah N.S., Inventor; Sherwood Medical Industries Inc., assignee. Medical Device for Collecting a Body Sample1982.

37. Milgrom H.T, Inventor; Milex Products, Inc., assignee. Tissue-Collecting Apparatus1983.

38. Kotsifas P.N., Wetzel V.H., Gilson W., Inventors; Sherwood Medical Company, assignee. Endometrial Sampling Device 1984.

39. Neuwirth R.S., Bolduc L.R., Inventors; Gynelab Products, assignee. Intrauterine Cauterizing Apparatus1990.

40. Anapliotis E., Inventor; Merete Management GmbH, assignee. Device for Taking a Biological or Cytological Smear 2003.

41. Gruber W.H., Inventor; Knobbe Martens Olson and Bear LLP, assignee. Systems, Methods, and Devices for Performing Gynecological Procedures 2008.

42. Alderete J.P., Castella P.C., Inventors; Xenotope Diagnostics, Inc., assignee. Method and Device for Trichomonas Detection 2008.

43. Lee-Sepsick K., Azevedo M.S., Currie D.S., Inventors. Methods and Devices for Conduit Occlusion 2009.

44. Patel MP, Patel RR, Patel JK. Chitosan Mediated Drug delivery System: A Review. *J Pharm Pharmaceut Sci* 2010;13(3):536-557.

45. Sampathkumar SG, Yarem KJ. Targeting Cancer Cells Dendrimer. *Chemistry & Biology.* 2005;12:5-13.

46. Duncan R. The Dawning Era of Polymer Therapeutic. *Nature Reviews Drug Discovery.* 2003;2:347-360.

47. Torchilin V. Antibody-modified liposomes for Cancer Chemotherapy. *Expert Opin. Drug Deliv.* 2008;5(9):1003-1025.

48. Zhang H, Oh M, Allen C, Kumacheva E. Monodisperse Chitosan Nanoparticles for Mucosal Drug Delivery. *Biomacromolecules.* 2004:2461-2468.

49. Xi-Peng G, Da-Ping Q, Kai-Rong L, Tao W, Peng X, Mai KC. Preparation and Characterization of Cationic Chitosan-modified Poly(D,L-lactide-co-glycolide) Copolymer Nanospheres as DNA Carriers. *J Biomater Appl.* 2007:353-370.

50. Goycoolea FM, Lollo G, Remunan-Lopez G, Quaglia F, Alonso MJ. Chitosan-Alginate Blended Nanoparticles as Carriers for the Transmucosal Delivery of Macromolecules. *Biomacromolecules.* 2009;10:1736-1743.

51. Zhang H, Wu S, Tao Y, Zang L, Su Z. Preparation and Characterization of Water-Soluble Chitosan Nanoparticles as Protein Delivery System. *Journal of Nanomaterials.* 2009;2010:1-5.

52. Racovita S, Vasiliu S, Popa M, Luca C. Polysaccharides based on micro- and nanoparticles obtained by ionic gelation and their application as drug delivery systems. *Revue Roumaine de Chimie.* 2009;54(9):709-718.

53. Janes KA, Clavo P, Alonso MJ. Polysaccharide colloidal particles as delivery systems for macromolecule. *Adv Drug Deliv Rev.* 2001;47:83-97.

54. Patel JK, Jivani NP. Chitosan Based Nanoparticles in Drug Delivery. *International Journal of Pharmaceutical Sciences and Nanotechnology.* 2009;2(2):517-522.

55. Muhammed R, Junise V, Saraswathi P, Krishnan P, Dilip C. Development and characterization of chitosan nanoparticles loaded with isoniazid for the treatment of Tuberculosis. *Reseach Journal of Pharmaceutical, Biological and Chemical Sciences.* 2010:383-390.

56. Phaechamud T, Charoenteeraboon J. Antibacterial Activity and Drug Release of the Chitosan Sponge Containing Hyclate. *AAPS PharmSciTech.* 2008;9(3):829-835.

57. Ko JA, Park HJ, Hwang SJ, Park JB, Lee JS. Preparation and Characterization of Chitosan Microparticles intended for Controlled Drug Delivery. *International Journal of Pharmaceutics.* 2002:165-174.

58. Sarmento B, Ribeiro A, Veiga F, Ferreira D. Development and characterization of new insulin containing polysaccharide nanoparticle. *Colloids and Surfaces B: Biointerface.* 2006;53:193-202.

59. Tokumitsu H, Ichikawa H, Fukumori Y. Chitosan-Gadopentetic Acid Complex Nanoparticles for Gadolinium Neutron-Capture Therapy Therapy of Cancer: Preparation by Novel Emulsion-Droplet Coalescence Technique and Characterization. *Pharmaceutical Research.* 1999;16(12):1830-1835.

60. Pawan P, Mayur M, Ashwin S. Role of Natural Polymers in Sustained Release Drug Delivery System: Application and Recent Approaches. *International Research Journal of Pharmacy.* 2011;2(9):6-11.

61. Liu Z, Jiao Y, Wang Y, Zhou C, Zhang Z. Polysaccharides-based nanoparticles as drug delivery systems. *Adv Drug Deliv Rev.* 2008;60:1650-1662.

62. Mohanraj VJ, Chen Y. Nanoparticle- A Review. *Tropical Journal of Pharmaceutical Research.* 2006;5(1):561-573.

63. Nicol S. Life after death for empty shells. *New Sci.* 1991;129:46-48.

64. Agnihotri SA, Mallikarjuna NN, Aminabhavi TM. Recent Advances on chitosan-based micro- and nanoparticles in drug delivery. *Journal of Controlled Release.* 2004;100:5-28.

65. Moghimi SM, Hunter AC, Murray JC. Long-circulating and target specific nanoparticles: theory to practice. *Pharmacol.Rev.* 2001;53(2):283-318.

66. Wang JJ, Zeng ZW, Xiao RZ, et al. Recent advances of chitosan nanoparticles as drug carriers. *International Journal of Nanomedicine.* 2011;6:765–774.

67. Tiyaboonchai W. Chitosan Nanoparticles : A Promising System for Drug Deliver. *Naresuan University Journal.* 2003;11(3):51-66.

68. Nagpal K, Kumar-Singh S, Nath-Mishr D. Chitosan Nanoparticles: A Promising System in Novel Drug Deliver. *Chem. Pharm. Bull.* 2010;58(11):1423-1430.

69. Grenha A, Seijo B, Serra C, Remunan-Lopez C. Chitosan Nanoparticle-Loaded Mannitol Microspheres: Structure and Surface Characterization. *Biomacromolecules.* 2007;8:2072-2079.

70. Shanmuganathan S, Shanumugasundaram N, Adhirajan N, Ramyaa-Lakshmi TS, Babu M. Preparation and characterization of chitosan microsphere for doxycycline delivery. *Carbohydrate Polymers.* 2007:201-211.

71. Pinto-Reis C, Neufeld RJ, Ribeiro AJ, Veiga F. Nanoencapsulation I. Methods for preparation of drug-loaded polymeric nanoparticles. *Nanomedicine.* 2006:8-21.

72. Clavo P, Vila-Jato J, Alonso MJ. Evalution of catonic polymer coated nanocapsules as ocular drug carriers. *Journal of Pharmaceutics.* 1997;153:41-50.

73. Mehrotra A, Nagarwal RC, Kumar-Pandit J. Lomustine Loaded Chitosan Nanoparticles: Characterization and in-Vitro Cytotoxicity on Human Lung Cancer Cell Line L13. *Chem. Pharm. Bull.* 2011;59(3):315-320.

74. Watzke HJ, Dieschbourg C. Novel silica-biopolymer nanocomposites: the silica sol-gel process in biopolymer organogels. *Advances in Colloid and Interface Science.* 1994;50:1-14.

75. Ohya Y, Shiratani M, Kobayashi H, Ouchi T. Release Behavior of 5-Fluorouracil from Chitosan-Gel Nanospheres Immobilizing 5-Fluorouracil Coated with Polysaccharides and Their Cell Specific Cytotoxicity. *Journal of Macromolecular Science.* 1994;31(5):629-642.

76. Bodmeier R, Chen H, Paeratakul O. A Novel Approach to the Delivery of Microparticles or Nanoparticles *Pharm Res.* 1989;6:413-417.

77. Shirashi S, Imani T, Ogtagiri M. Controlled release of indomethacin by chitosan-polyelectrolyte complex optization and in vivo: in vitro evaluation. *J. Control. Release.* 1993;25(3):217-225.

78. Clavo P, Remunan-Lopez C, Vila-Jata JL, Alonso MJ. Chitosan and Chitosan/Ethylene Oxide-Propylene Oxide Block Copolymer Nanoparticles as Novel Carrier for Protein and Vaccines. *Pharm Res.* 1997;14(10):1431-1436.

79. Gan Q, Wang T, Cochrane C, McCarron P. Modulation of surface charge, particle size and morphological properties of chitosan-TPP nanoparticles intended for gene delivery. *Colloids Surf. B Biointerfaces.* 2005;44:65-73.

80. Dung TH, Lee SR, Han SD, et al. Chitosan-TPP nanoparticles as a release system of antiense oligonucleotide in the oral environment. *J. Nanosci. Nanotechnol.* 2007;7(11):3695-3699.

81. Fernandez-Urrusuno R, Clavo P, Remunan-Lopez C, Vila-Jato JL, Alonso MJ. Enchancement of nasal absorption of insulin using chitosan nanoparticles. *Pharm. Res.* 1999;16:1576-1581.

82. Pan Y, Li Y, Zhao H, et al. Chitosan nanoparticles improve the intestinal absorption of insulin in vivo. *Int. J. Pharm.* 2002;249:139-147.

83. Shu XZ, Zhu KJ. A novel approach to prepare tripolyphospate/chitosan complex beads for controlled release drug delivery. *Int. J. Pharm.* 2000;201(1):51-58.

84. Xu Y, Du Y. Effect of molecular structure of chitosan on protein delvery properties of chitosan nanoparticles. *Int. J. Pharm.* 2003;250(1):215-226.

85. Boonsongrit Y, Mitrevej A, Mueller BW. Chitosan drug binding by ionic interaction. *European Journal of Pharmaceutics and Biopharmaceutics.* 2006;62:267-274.

86. Calvo P, Remunan-Lopez C, Vila-Jata JL, Alonso MJ. Novel Hydrophilic Chitosanpolyethylene Oxide Nanoparticles as Protein Carriers *J. Appl. Polym. Sci.* 1997;63(1):125-132.

87. Joshi N, Miller D. Doxycycline Revisited. *Arch Intern Med.* 1997;157.

88. Cover N, Lai-Yuen S, Parsons A, Kumar A. Synergetic effects of doxycycline-load chitosan nanoparticles for improving drug delivery and efficacy. *International Journal of Nanomedicine.* 2011;Accepted.

89. Riond J, Riviere J. Pharmacology and Toxicology of Doxycycline. *Vet Hum Toxicol.* 1988;30(5):431-443.

90. Cunha BA, Sibley CM, Ristuccia AM. Doxycycline. *Therapeutic Drug Monitoring.* 1982:115-135.

91. Cunha BA, Domenico P, Cunha CB. Pharmacodymanics of doxycycline. *Clinical Microbiology and Infection.* 2001;6(270-273).

92. Gencosmanoglu R, Kurtkaya-Yapicier O, Tiftikci A, Avsar E, Tozun N, Oran ES. Mid-esophageal ulceration and candidiasis-associated distal esophagitis as two distinct clinical patterns of tetracycline or doxycycline-induced esophageal injury. *J Clin Gastroenterol.* 2004;38(6):484-489.

93. Morris TJ, Davis TP. Doxycycline-induced esophageal ulceration in the U.S. Military service. *Mil Med.* 2000;165(4):316-319.

94. Tahan V, Sayrak H, Bayar N, Erer B, Tahan G, Dane F. Doxycycline-induced ulceration mimicking esophageal cancer. *Cases J.* 2008;1(1):144.

95. Smith K, Leyden JJ. Safety of Doxycycline and Minocycline: A Systematic Review. *Clinical Therapeutics.* 2005;27(9):1329-1342.

96. Heffner JE, Standerfer RJ, Torstveit J, Unruh L. Clinical efficacy of Doxycycline for Pleurodesis. *Chest.* 1994;105(6):1743-1747.

97. Mansson T. Treatment of malignant pleural effusion with doxycycline. *Scand J Infect Dis Suppl.* 1988;53:29-34.

98. Robinson LA, Fleming WH, Galgraith TA. Intrapleural doxycycline control of malignant pleural effusions. *Ann Thorac Surg.* 1993;55:1115-1122.

99. Hurewitz AN, Lidonicci K, Wu CL, Zucker S. Histologic changes of doxycycline pleurodesis in rabbits. Effect of concentration and pH. *Chest.* 1994;106(4):1241-1245.

100. Pulsiripunya C, Youngchaiyud P, Pushpakom R, Maranetra N, Nana A, Charoenratanakul S. The efficacy of doxycycline as a pleural sclerosing agent in malignant pleural effusion: a prospective study. *Respisology.* 1996;1(1):69-72.

101. Chien Y. *Novel Drug Delivery Systems.* Vol 50. New York Marcel Dekker; 1992.

102. Weisberg S. *Applied Linear Regression*. 2nd ed. New York: John Wiley; 1985.

103. Nellåker C, Uhrzander F, Tyrcha J, Karlsson H. Mixture models for analysis of melting temperature dat. *BMC Bioinformatics.* 2008;9:1-6.

104. Anderson DR, Burnham KP, Thompson WL. Null Hypothesis Testing: Problems, Prevalence, and An Alternative. *Journal of Wildlife Management.* 2000;64(4):912-923.

105. Burnham KP, Anderson DR. Kullback-Leibler Information as a Basis for Strong Inference in Ecological Studies. *Wildlife Research.* 2001;28:111-119.

106. Blanchet FG, Legendre P, Borcard D. Forward Selection of Explanatory Variables. *Ecology.* 2008;89:2623-2632.

107. Alameh M, Jean M, DeJesus D, Buschmann MD, Merzouk A. Chitosanase-based method for RNA isolation from cells transfected with chitosan/siRNA nanocomplexes for real-time RT-PCR in gene silencing. *International Journal of Nanomedicine.* 2010;5:473-481.

108. Lee YS, Jang KA, Cha JD. Synergistic Antibacterial Effect between Silibinin and Antibiotics in Oral Bacteria. *Journal of Biomedicine Biotechnology.* 2011:1-7.

Appendices

Appendix A: A Copy of the Pre-Development Survey

I. Purpose of survey**:** A Research group from the University of South Florida is conducting a prescreening survey about the development of a new medical device. The research group will use the data from this survey as the criteria for device development.

II. Targeted end-users: Obstetricians and Gynecologists

III. Proposed device function: To collect uncontaminated endometrium samples

IV. Your participation is important: Participation in this survey is voluntary. However, your cooperation is essential to the accuracy in prioritizing the criteria used for device development. The data reported on the questionnaire will be used for statistical purposes in ranking criteria.

Questions:

1. Are there presently any devices used to collect uncontaminated specimen from the uterus?
    a. Yes
    b. No
2. Rate the following criteria in order of importance on a scale of 1-5, with 1, being the most important to 5, the least:
    a. Comfort to patient
    b. Prevent contamination
    c. Ease of handling
    d. Device Durability
    e. Dimension of device
3. What is the major problem/difficulty in collecting uncontaminated specimen from the uterus?
    a. No proven device is available
    b. Avoiding contamination by vaginal flora
    c. Painful procedure for the patient
    d. Laboratory wont identified organisms beyond the “normal genital flora”
    e. Other
4. What type of sampler, do you currently use for endometrium biopsy?
    a. SelectCell
    b. SelectCell Mini
    c. Pipelle
    d. Tao Brush
    e. Milex Pipet Curet
    f. Uterine Explora Model 1
    g. Other
5. Do you think there is need for a device that will collect uncontaminated uterine samples to diagnose possible uterine diseases?
    a. Yes
    b. No

Appendix B: List of the 64 Formulations of Chitosan Nanoparticles

Each formulation was done in triple and then all three trials were averaged. The average particle size is represented in the last column.

F	CS_TYPE	CS_CONC	CS_SOLV	PRO_TIME	TPP_CONC	TPP_SOLV	DRUG	ORDER	RATIO	SYN_TIME	CENTRI	REC_SOLV	AVERAGE PAR_SIZE
1	0	0.2	0	60	0.84	0	1	0	4	60	1	1	90
2	0	0.2	0	60	0.84	0	1	0	4	60	1	1	155
3	0	0.1	0	60	0.21	0	0	1	4	60	1	1	33
4	0	0.1	0	60	0.42	0	0	1	4	60	1	1	114
5	0	0.1	0	30	0.42	0	0	1	4	120	0	1	99.5
6	0	0.1	0	30	0.42	0	0	1	4	1440	0	1	415
7	0	0.1	0	30	0.42	0	0	1	4	60	0	1	142
8	0	0.2	0	60	0.84	0	1	1	4	1440	1	1	3486
9	0	0.1	0	60	0.42	0	1	1	4	1440	1	1	4905
10	1	0.2	1	1440	0.84	1	1	0	2	60	1	0	102
11	1	0.2	1	1440	0.84	1	1	0	2	60	1	0	143
12	1	0.2	1	1440	0.84	1	1	0	2	60	0	0	169.5
13	0	0.2	1	1440	0.84	1	1	0	2	60	1	0	427
14	0	0.2	1	1440	0.84	1	1	0	1	60	1	0	320
15	0	0.2	1	1440	0.84	1	1	1	2	60	1	0	620
16	1	0.2	1	1440	0.84	1	1	0	1	60	1	0	600
17	0	0.2	1	1440	0.84	1	1	0	1	60	1	1	4000
18	1	0.2	1	1440	0.84	1	1	0	1	60	0	1	4000
19	0	0.2	1	1440	0.84	1	1	0	1	120	0	1	6000
20	1	0.2	1	1440	0.84	1	1	0	1	120	0	1	3550
21	0	0.2	1	1440	0.84	1	1	0	1	120	1	1	4450
22	1	0.2	1	1440	0.84	1	1	0	1	120	1	1	5700
23	0	0.2	1	1440	0.84	1	1	1	2	120	0	1	575
24	1	0.2	1	1440	0.84	1	1	1	2	120	0	1	2000
25	0	0.2	1	1440	0.84	1	1	1	2	60	0	0	595
26	0	0.2	1	1440	0.42	1	1	1	2	60	0	0	265
27	0	0.2	1	1440	0.84	1	1	0	2	60	0	0	3250
28	0	0.2	1	1440	0.42	1	1	0	2	60	0	0	4000
29	1	0.2	1	1440	0.84	1	1	1	2	60	0	0	3500
30	1	0.2	1	1440	0.84	1	1	0	2	60	0	0	3175
31	1	0.2	1	1440	0.42	1	1	1	2	60	1	0	70
32	1	0.2	1	1440	0.42	1	1	0	2	60	0	0	3750
33	0	0.2	1	1440	0.75	1	1	1	2	60	0	0	685
34	0	0.2	1	1440	0.6	1	1	1	2	60	0	0	255
35	1	0.2	1	1440	0.75	1	1	1	2	60	0	0	1500
36	1	0.2	1	1440	0.6	1	1	1	2	60	0	0	675
37	1	0.1	1	60	0.42	0	0	1	1	60	1	0	5450
38	1	0.1	1	60	0.42	0	0	1	1	60	0	0	3500
39	1	0.1	1	60	0.42	0	1	1	1	60	1	0	4000
40	1	0.1	1	60	0.42	0	1	1	1	60	0	0	4250
41	1	0.2	1	60	0.42	0	0	1	1	60	1	0	5000
42	1	0.2	1	60	0.42	0	0	1	1	60	0	0	4000
43	1	0.2	1	60	0.42	0	1	1	1	60	1	0	3500
44	1	0.2	1	60	0.42	0	1	1	1	60	0	0	2500
45	1	0.1	0	60	0.42	0	0	1	1	60	1	0	4050
46	1	0.1	0	60	0.42	0	0	1	1	60	0	0	4050
47	1	0.1	0	60	0.42	0	1	1	1	60	1	0	3750
48	1	0.1	0	60	0.42	0	1	1	1	60	0	0	2600
49	1	0.2	0	60	0.42	0	0	1	1	60	1	0	2545
50	1	0.2	0	60	0.42	0	0	1	1	60	0	0	2550
51	1	0.2	0	60	0.42	0	1	1	1	60	1	0	3550
52	1	0.2	0	60	0.42	0	1	1	1	60	0	0	1600
53	1	0.1	1	1440	0.42	0	0	1	1	60	1	1	3000
54	1	0.1	1	1440	0.42	0	0	1	1	60	0	1	3950
55	1	0.1	1	1440	0.42	0	1	1	1	60	1	1	5000
56	1	0.1	1	1440	0.42	0	1	1	1	60	0	1	6000
57	1	0.2	1	1440	0.42	0	0	1	1	60	1	1	950
58	1	0.2	1	1440	0.42	0	0	1	1	60	0	1	5500
59	1	0.2	1	1440	0.42	0	1	1	1	60	1	1	5550
60	1	0.2	1	1440	0.42	0	1	1	1	60	0	1	5050
61	1	0.1	1	1440	0.42	1	0	1	1	60	1	1	5000
62	1	0.1	1	1440	0.42	1	0	1	1	60	0	1	4100
63	1	0.1	1	1440	0.42	1	1	1	1	60	1	1	5900
64	1	0.1	1	1440	0.42	1	1	1	1	60	0	1	5300

Appendix C: AIC-Based Stepwise Selection Conditional Tests

AIC-based stepwise forward selection (RDA)							
Conditional Tests: (each variable separately)							
RSS	**R^2**	**R^2adj**	**AIC**	**Wts**	**Delta**	**Ratio**	**Variables**
1.7401e^{+08}	0.3105	0.2994	952.4053	0	0.9958	1	Chitosan:TPP Ratio
2.0692e^{+08}	0.1802	0.1669	963.4904	11.0851	0.0039	255.3269	Chitosan Type
2.3345e^{+08}	0.0750	0.0601	971.2121	18.8068	8.2099e^{-05}	1.2129e^{+04}	TPP Concentration
2.3659e^{+08}	0.0626	0.0475	972.0659	19.6606	5.3571e^{-05}	1.8589e^{+04}	Chitosan Concentration
2.3771e^{+08}	0.0582	0.0430	972.3683	19.9630	4.6054e^{-05}	2.1623e^{+04}	Wash/Reconstitution Solution
2.3964e^{+08}	0.0505	0.0352	972.8854	20.4801	3.5562e^{-05}	2.8002e^{+04}	Chitosan Dissolving Solution
2.5239e^{+08}	NaN	NaN	974.0718	21.6665	1.9650^{e-05}	5.0678e^{+04}	None
2.4539e^{+08}	0.0277	0.0121	974.4036	21.9983	1.6646e^{-05}	5.9823e^{+04}	TPP Dissolving solution
2.4995e^{+08}	0.0097	-0.0063	975.5816	23.1763	9.2365e^{-06}	1.0781e^{+05}	Order
2.5196e^{+08}	0.0017	-0.0144	976.0933	23.6880	7.1515e^{-06}	1.3925e^{+05}	Protonation Time
2.5203e^{+08}	0.0014	-0.0147	976.1125	23.7072	7.0832e^{-06}	1.4059e^{+05}	Drug
2.5222e^{+08}	6.6606e^{-04}	-0.0155	976.1614	23.7561	6.9121e^{-06}	1.4407e^{+05}	Synthesis Time
2.5239e^{+08}	5.0692e^{-07}	-0.0161	976.2040	23.7987	6.7664e^{-06}	1.4717e^{+05}	Centrifugation

Appendix D: AIC-Based Stepwise Selection Marginal Tests

AIC-based stepwise forward selection (RDA)						
Marginal Tests: (sequential variable addition)						
RSS	**R^2**	**R^2adj**	**AIC**	**Wts**	**DeltaN**	**Variables**
1.7401e^{+08}	0.3105	0.2994	952.4053	0.9958	21.6665	Ratio
1.3499e^{+08}	0.4652	0.4476	938.3569	0.8535	14.0484	Wash/Reconstitution Solution
1.1456e^{+08}	0.5461	0.5234	930.1306	0.7613	8.2263	Synthesis Time
1.0698e^{+08}	0.5761	0.5474	928.1074	0.2282	2.0232	TPP Concentration
1.0698e^{+08}	NaN	NaN	928.1074	0.2034	0	None

Appendix E: Stepwise Redundancy Analysis Global Test

Stepwise REDUNDANCY ANALYSIS			
Global Test: (all variables included)			
F	**p**	**R^2**	**R^2adj**
7.7013	$1.0000e^{-03}$	0.6444	0.5607

Appendix F: Stepwise Redundancy Analysis Conditional Tests

Stepwise REDUNDANCY ANALYSIS				
Conditional Tests: (each variable separately)				
F	**p**	**R^2**	**R^2adj**	**Variables**
13.6248	$1.0000e^{-03}$	0.1802	0.1669	Chitosan Type
4.1412	0.0540	0.0626	0.0475	Chitosan Concentration
3.2997	0.0790	0.0505	0.0352	Chitosan Dissolving Solution
0.1074	0.7450	0.0017	-0.0144	Protonation Time
5.0296	0.0330	0.0750	0.0601	TPP Concentration
1.7689	0.1870	0.0277	0.0121	TPP Dissolving solution
0.0887	0.7730	0.0014	-0.0147	Drug
0.6059	0.4250	0.0097	-0.0063	Order
27.9262	$1.0000e^{-03}$	0.3105	0.2994	Ratio
0.0413	0.8440	$6.6606e^{-04}$	-0.0155	Synthesis Time
$3.1429e^{-05}$	0.9950	$5.0692e^{-07}$	-0.0161	Centrifugation
3.8295	0.0520	0.0582	0.0430	Wash/Reconstitution Solution

Appendix G: Stepwise Redundancy Analysis Marginal Tests

Stepwise REDUNDANCY ANALYSIS					
Marginal Tests: (sequential variable addition)					
Partial F	**P**	**Partial R^2**	**Partial R^2adj**	**Cum R^2adj**	**Variables**
27.9262	$1.0000e^{-03}$	0.3105	0.2994	0.2994	Ratio
17.6342	$1.0000e^{-03}$	0.1546	0.1410	0.4476	Wash/Reconstitution Solution
10.7019	0.0030	0.0810	0.0661	0.5234	Synthesis Time
4.1789	0.0500	0.0300	0.0144	0.5474	TPP Concentration

Appendix H: Multiple Linear Regression via QR Factorization

Multiple Linear Regression via QR Factorization				
R^2	**R^2adj**	**F-stat**	**Para-p**	**Perm-p**
0.57614	0.54740	20.04913	0.00000	0.00100

Multiple Linear Regression via QR Factorization				
Variables	**b**	**t-stat**	**Parametric-p**	**Permutation-p**
Intercept	6820.73439	11.24915	0.00000	0.00200
1	-1520.19243	-7.86486	0.00000	0.00200
2	-1383.24087	-3.89756	0.00024	0.00200
3	2.19529	3.23940	0.00191	0.00200
4	-1714.64471	-2.04425	0.04511	0.02400

Appendix I: Doxycycline Standard Curve

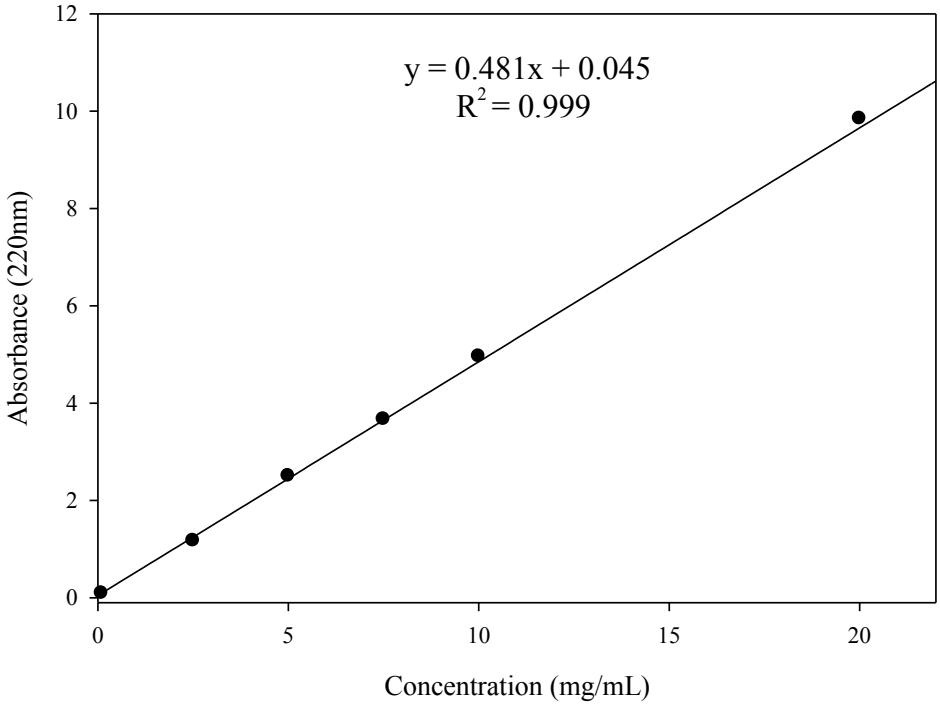

Appendix J: Hek 293 Transfected Cells with pGFP

Shows the expression of pGFP in Hek 293 cells after transfected with pGFP-loaded chitosan nanoparticles prepared using the ionic gelation method day 3.

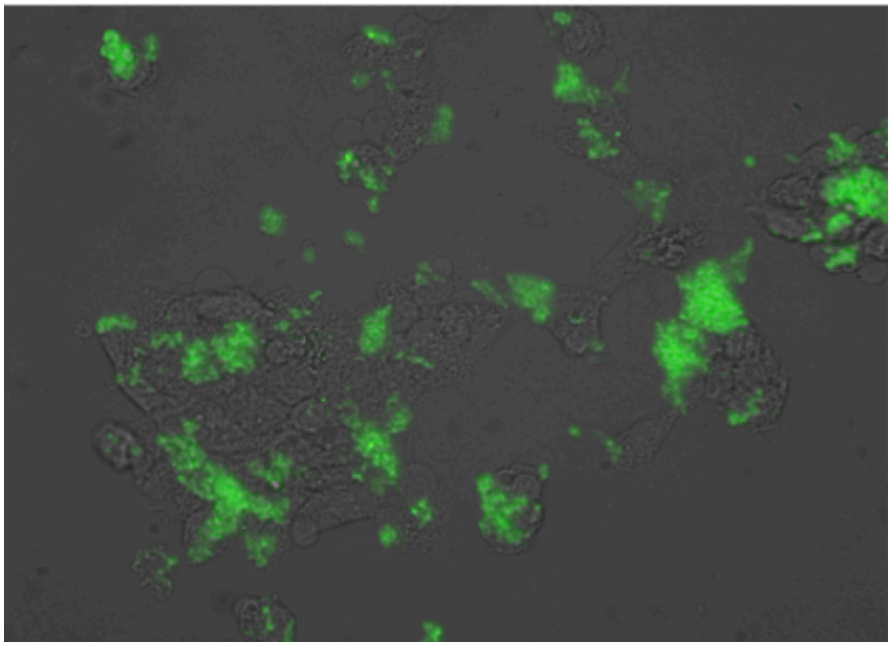

Appendix K: Day 1 WST-1 Raw Data for Formulation 1

	1	2	3	4	5	6	7	8	9	10	11	12	
A	0.278	0.287	0.261	0.58	0.626	0.621	0.976	1.009	0.914	1.703	1.766	1.814	450
B	0.275	0.3	0.299	0.297	0.294	0.303	0.282	0.288	0.29	0.291	0.287	0.227	450
C	0.379	0.378	0.427	0.55	0.628	0.567	0.871	0.915	0.953	0.282	0.285	0.28	450
D	0.405	0.384	0.384	0.485	0.524	0.65	0.719	0.792	0.158	0.799	0.654	0.64	450
E	0.512	0.537	0.653	1.035	0.953	1.02	1.47	1.546	1.451	0.809	0.9	0.86	450
F	0.597	0.532	0.525	0.884	0.892	0.946	1.557	1.519	1.488	1.377	1.651	1.47	450
G	0.048	0.05	0.047	0.047	0.047	0.05	0.047	0.048	0.047	0.047	0.047	0.046	450
H	0.048	0.048	0.048	0.047	0.047	0.046	0.046	0.046	0.047	0.047	0.047	0.046	450

	1	2	3	4	5	6	7	8	9	10	11	12	
A	0.184	0.19	0.173	0.293	0.312	0.309	0.442	0.462	0.448	0.763	0.752	0.785	490
B	0.179	0.196	0.196	0.194	0.193	0.198	0.187	0.19	0.191	0.191	0.189	0.152	490
C	0.225	0.229	0.235	0.271	0.277	0.283	0.369	0.38	0.386	0.186	0.188	0.185	490
D	0.237	0.232	0.226	0.266	0.271	0.303	0.333	0.346	0.106	0.411	0.328	0.339	490
E	0.274	0.283	0.333	0.462	0.433	0.45	0.626	0.689	0.669	0.402	0.426	0.434	490
F	0.313	0.287	0.283	0.415	0.434	0.452	0.669	0.673	0.669	0.556	0.701	0.678	490
G	0.046	0.047	0.044	0.044	0.044	0.048	0.044	0.045	0.044	0.044	0.045	0.045	490
H	0.045	0.045	0.046	0.045	0.045	0.044	0.044	0.044	0.044	0.044	0.044	0.044	490

	1	2	3	4	5	6	7	8	9	10	11	12	
A	0.051	0.051	0.047	0.049	0.05	0.05	0.051	0.053	0.052	0.054	0.055	0.053	630
B	0.051	0.053	0.052	0.05	0.053	0.053	0.053	0.052	0.05	0.05	0.05	0.046	630
C	0.053	0.054	0.053	0.054	0.054	0.053	0.056	0.058	0.056	0.05	0.05	0.05	630
D	0.055	0.054	0.053	0.055	0.055	0.056	0.056	0.057	0.042	0.068	0.052	0.053	630
E	0.05	0.051	0.053	0.054	0.052	0.053	0.056	0.057	0.057	0.054	0.055	0.053	630
F	0.054	0.059	0.052	0.052	0.055	0.054	0.054	0.055	0.056	0.052	0.056	0.055	630
G	0.043	0.045	0.041	0.041	0.043	0.045	0.042	0.042	0.041	0.042	0.043	0.043	630
H	0.043	0.042	0.042	0.042	0.044	0.043	0.042	0.041	0.043	0.041	0.043	0.041	630

Appendix L: Day 3 WST-1 Raw Data for Formulation 1

	1	2	3	4	5	6	7	8	9	10	11	12	
A	0.292	0.304	0.313	1.078	1.02	0.956	1.473	1.398	1.22	0.522	0.535	0.53	450
B	0.312	0.319	0.331	0.328	0.326	0.297	0.297	0.31	0.297	0.323	0.309	0.33	450
C	0.399	0.41	0.389	0.421	0.454	0.613	0.607	0.59	0.67	0.31	0.326	0.334	450
D	0.372	0.393	0.37	0.399	0.371	0.373	0.447	0.463	0.47	1.062	0.938	1.057	450
E	0.99	1.193	1.094	1.543	1.532	1.549	1.494	1.594	1.891	1.468	1.3	1.341	450
F	1.143	1.163	1.183	1.584	1.805	1.555	1.26	1.155	1.097	1.424	0.813	1.042	450
G	0.056	0.049	0.047	0.047	0.047	0.059	0.047	0.047	0.051	0.047	0.047	0.047	450
H	0.047	0.049	0.047	0.047	0.046	0.046	0.047	0.047	0.047	0.056	0.047	0.046	450

	1	2	3	4	5	6	7	8	9	10	11	12	
A	0.183	0.19	0.192	0.497	0.494	0.481	0.675	0.658	0.591	0.271	0.275	0.275	490
B	0.193	0.196	0.201	0.198	0.197	0.19	0.19	0.195	0.192	0.202	0.188	0.2	490
C	0.248	0.233	0.223	0.23	0.241	0.311	0.279	0.287	0.309	0.195	0.204	0.204	490
D	0.222	0.225	0.219	0.226	0.217	0.221	0.238	0.252	0.251	0.444	0.419	0.511	490
E	0.455	0.484	0.468	0.663	0.648	0.642	0.657	0.702	0.754	0.641	0.587	0.634	490
F	0.517	0.502	0.522	0.683	0.726	0.649	0.535	0.513	0.493	0.612	0.383	0.495	490
G	0.054	0.047	0.044	0.044	0.044	0.057	0.045	0.045	0.048	0.045	0.045	0.045	490
H	0.044	0.046	0.045	0.045	0.044	0.045	0.045	0.045	0.045	0.053	0.044	0.044	490

	1	2	3	4	5	6	7	8	9	10	11	12	
A	0.048	0.05	0.046	0.051	0.051	0.05	0.056	0.057	0.055	0.055	0.053	0.054	630
B	0.049	0.051	0.05	0.048	0.048	0.049	0.049	0.049	0.047	0.049	0.048	0.05	630
C	0.077	0.053	0.052	0.051	0.05	0.061	0.052	0.053	0.051	0.049	0.052	0.05	630
D	0.054	0.052	0.052	0.052	0.053	0.052	0.049	0.053	0.053	0.051	0.051	0.054	630
E	0.053	0.052	0.051	0.054	0.055	0.054	0.057	0.062	0.063	0.057	0.057	0.056	630
F	0.055	0.052	0.051	0.057	0.056	0.054	0.058	0.069	0.062	0.057	0.058	0.06	630
G	0.049	0.044	0.041	0.041	0.043	0.054	0.043	0.042	0.044	0.043	0.043	0.043	630
H	0.041	0.042	0.041	0.042	0.043	0.043	0.042	0.042	0.042	0.05	0.042	0.042	630

Appendix M: Day 5 WST-1 Raw Data for Formulation 1

	1	2	3	4	5	6	7	8	9	10	11	12	
A	0.458	0.464	0.438	1.268	1.065	1.044	0.631	0.564	0.609	0.869	0.935	0.842	450
B	0.474	0.462	0.38	0.4	0.423	0.382	0.429	0.409	0.423	0.424	0.445	0.436	450
C	0.52	0.489	0.428	0.422	0.455	0.432	0.503	0.495	0.491	0.44	0.451	0.384	450
D	0.527	0.46	0.441	0.442	0.433	0.445	0.429	0.484	0.461	1.649	1.311	1.446	450
E	1.697	1.997	1.652	1.475	1.384	1.441	1.366	1.292	1.166	1.393	0.864	1.402	450
F	1.872	1.871	1.696	0.925	1.624	2.019	1.05	1.057	0.937	0.868	0.864	0.904	450
G	0.047	0.047	0.049	0.048	0.047	0.047	0.047	0.047	0.047	0.049	0.048	0.046	450
H	0.049	0.047	0.049	0.046	0.048	0.046	0.046	0.046	0.046	0.048	0.048	0.049	450

	1	2	3	4	5	6	7	8	9	10	11	12	
A	0.281	0.279	0.263	0.64	0.536	0.565	0.356	0.307	0.338	0.492	0.538	0.422	490
B	0.287	0.281	0.257	0.25	0.255	0.247	0.262	0.254	0.262	0.267	0.262	0.265	490
C	0.31	0.289	0.281	0.251	0.281	0.281	0.295	0.291	0.287	0.27	0.274	0.229	490
D	0.319	0.299	0.271	0.289	0.27	0.278	0.255	0.293	0.286	0.664	0.587	0.672	490
E	0.768	0.865	0.722	0.656	0.672	0.624	0.611	0.571	0.53	0.614	0.43	0.656	490
F	0.841	0.815	0.757	0.459	0.712	0.862	0.481	0.505	0.467	0.441	0.441	0.445	490
G	0.045	0.045	0.046	0.045	0.045	0.045	0.045	0.045	0.045	0.046	0.046	0.044	490
H	0.046	0.044	0.046	0.044	0.046	0.044	0.044	0.044	0.044	0.045	0.045	0.047	490

	1	2	3	4	5	6	7	8	9	10	11	12	
A	0.059	0.056	0.053	0.065	0.068	0.068	0.068	0.063	0.059	0.119	0.144	0.061	630
B	0.059	0.059	0.055	0.053	0.055	0.054	0.056	0.057	0.055	0.055	0.056	0.055	630
C	0.062	0.059	0.058	0.052	0.057	0.058	0.06	0.06	0.058	0.056	0.058	0.051	630
D	0.064	0.063	0.06	0.061	0.059	0.056	0.057	0.06	0.062	0.061	0.065	0.06	630
E	0.065	0.067	0.066	0.072	0.07	0.071	0.083	0.059	0.082	0.072	0.07	0.068	630
F	0.065	0.066	0.064	0.069	0.064	0.061	0.054	0.057	0.059	0.061	0.068	0.071	630
G	0.041	0.043	0.042	0.043	0.043	0.042	0.043	0.042	0.041	0.044	0.043	0.043	630
H	0.044	0.04	0.043	0.041	0.044	0.043	0.042	0.041	0.041	0.041	0.043	0.043	630

Appendix N: Day 1 WST-1 Raw Data for Formulation 2

1	2	3	4	5	6	7	8	9	10	11	12	
0.148	0.179	0.191	0.835	0.851	0.83	0.838	1.006	0.796	1.613	1.668	1.58	450
0.195	0.181	0.192	0.207	0.202	0.207	0.206	0.197	0.196	0.202	0.197	0.195	450
0.557	0.632	0.627	0.636	0.642	0.595	0.951	0.994	0.957	0.196	0.189	0.198	450
0.497	0.473	0.491	0.492	0.524	0.5	0.828	0.739	0.648	0.83	0.72	0.663	450
0.676	0.805	0.749	0.723	0.766	0.72	1.408	1.142	1.28	0.916	0.734	0.711	450
0.612	0.529	0.66	0.666	0.758	0.694	1.111	1.136	1.05	1.241	1.538	1.109	450
0.047	0.047	0.047	0.047	0.047	0.047	0.047	0.047	0.053	0.047	0.047	0.047	450
0.047	0.047	0.047	0.046	0.047	0.046	0.047	0.047	0.046	0.047	0.047	0.047	450

1	2	3	4	5	6	7	8	9	10	11	12	
0.106	0.126	0.134	0.392	0.393	0.385	0.409	0.457	0.375	0.666	0.712	0.668	490
0.134	0.127	0.136	0.143	0.14	0.142	0.149	0.141	0.14	0.142	0.14	0.143	490
0.263	0.288	0.301	0.312	0.304	0.292	0.412	0.416	0.442	0.14	0.136	0.142	490
0.258	0.248	0.252	0.264	0.265	0.253	0.373	0.347	0.312	0.388	0.337	0.326	490
0.311	0.354	0.341	0.326	0.35	0.327	0.589	0.517	0.557	0.426	0.345	0.351	490
0.296	0.249	0.325	0.325	0.358	0.336	0.47	0.525	0.465	0.538	0.649	0.478	490
0.045	0.045	0.044	0.044	0.044	0.045	0.044	0.044	0.051	0.045	0.045	0.044	490
0.044	0.045	0.044	0.044	0.044	0.044	0.045	0.044	0.044	0.044	0.044	0.044	490

1	2	3	4	5	6	7	8	9	10	11	12	
0.039	0.039	0.038	0.042	0.041	0.041	0.045	0.046	0.041	0.043	0.045	0.045	630
0.04	0.04	0.04	0.039	0.04	0.041	0.048	0.04	0.04	0.039	0.039	0.041	630
0.042	0.042	0.042	0.042	0.042	0.041	0.044	0.043	0.044	0.04	0.039	0.041	630
0.043	0.042	0.042	0.044	0.044	0.042	0.043	0.043	0.045	0.044	0.042	0.041	630
0.041	0.042	0.042	0.043	0.041	0.041	0.043	0.044	0.045	0.043	0.042	0.042	630
0.041	0.043	0.044	0.042	0.046	0.043	0.043	0.054	0.044	0.044	0.044	0.045	630
0.043	0.042	0.041	0.042	0.043	0.042	0.042	0.041	0.048	0.043	0.042	0.043	630
0.042	0.04	0.041	0.041	0.042	0.042	0.042	0.041	0.041	0.042	0.042	0.042	630

Appendix O: Day 3 WST-1 Raw Data for Formulation 2

	1	2	3	4	5	6	7	8	9	10	11	12	
A	0.186	0.189	0.191	1.621	1.837	2.17	1.789	2.469	2.908	2.321	2.086	2.275	450
B	0.259	0.278	0.274	0.292	0.28	0.286	0.275	0.272	0.265	0.273	0.281	0.265	450
C	1.161	0.965	0.962	0.944	1.28	1.154	1.708	1.616	1.348	0.277	0.271	0.28	450
D	0.404	0.461	0.495	0.471	0.578	0.57	0.747	0.833	0.886	1.488	1.93	1.425	450
E	1.941	1.812	2.135	1.526	1.658	1.68	2.705	2.63	2.918	1.626	1.878	1.437	450
F	0.907	1.081	1.025	0.69	0.965	0.922	1.735	1.408	1.537	2.07	1.815	2.013	450
G	0.048	0.047	0.061	0.048	0.047	0.047	0.047	0.05	0.049	0.052	0.047	0.048	450
H	0.047	0.046	0.047	0.049	0.047	0.05	0.046	0.047	0.047	0.048	0.047	0.047	450

	1	2	3	4	5	6	7	8	9	10	11	12	
A	0.132	0.134	0.135	0.765	0.775	0.847	0.831	0.938	0.939	0.902	0.854	0.955	490
B	0.171	0.187	0.183	0.194	0.184	0.19	0.19	0.186	0.182	0.187	0.192	0.181	490
C	0.515	0.425	0.472	0.381	0.5	0.436	0.607	0.555	0.562	0.189	0.183	0.194	490
D	0.227	0.245	0.24	0.244	0.262	0.284	0.339	0.329	0.359	0.591	0.796	0.628	490
E	0.764	0.742	0.808	0.597	0.656	0.755	1.041	1.079	1.192	0.714	0.788	0.641	490
F	0.399	0.444	0.419	0.331	0.42	0.393	0.759	0.601	0.647	0.88	0.792	0.874	490
G	0.045	0.045	0.057	0.045	0.045	0.045	0.045	0.047	0.046	0.05	0.046	0.046	490
H	0.044	0.044	0.044	0.046	0.044	0.047	0.044	0.044	0.046	0.045	0.045	0.045	490

	1	2	3	4	5	6	7	8	9	10	11	12	
A	0.04	0.04	0.039	0.045	0.044	0.048	0.049	0.047	0.047	0.051	0.054	0.053	630
B	0.042	0.043	0.042	0.041	0.042	0.042	0.044	0.043	0.042	0.042	0.042	0.042	630
C	0.046	0.045	0.047	0.046	0.045	0.044	0.05	0.05	0.048	0.042	0.043	0.043	630
D	0.043	0.045	0.044	0.044	0.047	0.042	0.045	0.044	0.055	0.058	0.048	0.046	630
E	0.047	0.046	0.047	0.045	0.044	0.047	0.052	0.057	0.052	0.056	0.047	0.046	630
F	0.046	0.048	0.05	0.046	0.045	0.045	0.05	0.051	0.053	0.055	0.054	0.048	630
G	0.043	0.042	0.051	0.043	0.043	0.042	0.043	0.044	0.043	0.046	0.043	0.044	630
H	0.043	0.04	0.04	0.044	0.043	0.045	0.041	0.041	0.041	0.043	0.042	0.043	630

Appendix P: Day 5 WST-1 Raw Data for Formulation 2

	1	2	3	4	5	6	7	8	9	10	11	12	
A	0.401	0.395	0.389	1.246	0.87	1.186	0.921	0.85	0.812	1.202	1.04	0.927	450
B	0.389	0.393	0.376	0.38	0.382	0.38	0.362	0.372	0.361	0.363	0.373	0.353	450
C	0.825	0.834	0.82	0.785	0.815	0.962	1.085	0.989	0.842	0.375	0.379	0.381	450
D	0.423	0.435	0.431	0.44	0.43	0.448	0.587	0.461	0.467	1.271	3.073	2.811	450
E	2.572	2.343	2.432	2.172	2.324	2.223	2.326	0.815	0.965	1.169	1.25	1.088	450
F	1.358	1.442	1.141	1.474	1.525	1.29	1.262	0.874	1.198	1.173	0.868	1.012	450
G	0.047	0.048	0.048	0.047	0.05	0.048	0.057	0.049	0.062	0.048	0.048	0.048	450
H	0.047	0.048	0.047	0.048	0.047	0.047	0.051	0.047	0.047	0.047	0.047	0.048	450

	1	2	3	4	5	6	7	8	9	10	11	12	
A	0.273	0.269	0.267	0.54	0.402	0.482	0.456	0.449	0.43	0.598	0.551	0.477	490
B	0.274	0.274	0.259	0.26	0.263	0.261	0.255	0.262	0.254	0.256	0.262	0.242	490
C	0.401	0.419	0.409	0.441	0.405	0.438	0.503	0.618	0.464	0.266	0.268	0.27	490
D	0.288	0.284	0.304	0.299	0.299	0.294	0.33	0.304	0.305	0.609	1.401	1.23	490
E	0.989	1.913	1.953	1.904	2.059	2.047	1.114	0.515	0.53	0.518	0.663	0.541	490
F	0.652	0.696	0.571	0.571	0.684	0.503	0.757	0.503	0.644	0.603	0.498	0.522	490
G	0.044	0.045	0.045	0.045	0.044	0.045	0.053	0.046	0.058	0.045	0.046	0.045	490
H	0.044	0.045	0.045	0.045	0.044	0.045	0.048	0.045	0.045	0.044	0.044	0.045	490

	1	2	3	4	5	6	7	8	9	10	11	12	
A	0.044	0.045	0.044	0.05	0.049	0.051	0.054	0.055	0.05	0.059	0.061	0.059	630
B	0.046	0.047	0.045	0.044	0.045	0.047	0.047	0.047	0.045	0.045	0.044	0.044	630
C	0.049	0.049	0.049	0.048	0.049	0.049	0.052	0.051	0.052	0.047	0.046	0.046	630
D	0.048	0.049	0.049	0.05	0.05	0.047	0.048	0.051	0.052	0.052	0.05	0.052	630
E	0.053	0.076	0.057	0.058	0.084	0.086	0.066	0.061	0.061	0.056	0.056	0.055	630
F	0.049	0.048	0.049	0.055	0.052	0.05	0.058	0.064	0.059	0.059	0.059	0.053	630
G	0.042	0.042	0.041	0.042	0.042	0.042	0.049	0.044	0.053	0.043	0.043	0.044	630
H	0.043	0.041	0.041	0.043	0.042	0.043	0.044	0.042	0.04	0.043	0.042	0.043	630

About the Author

Natasha Faith Cover is the daughter of Neville Cover and Faith Smith. She attended the High School for Health and Human Services located in New York, New York. After graduating from high school, she enrolled at Virginia Union University where she received her Bachelor's of Science in Biology, and participated in the NIH Minority Access to Research Careers (MARC U STAR) and NSF Mid-Eastern LSAMP programs. She obtained her Master of Science degree in Biomedical Engineering from the University of South Florida, and is completing her doctoral degree. Natasha has been supported by the National Science Foundation Florida Georgia LSAMP Bridge to the Doctorate Fellowship, Florida Education Fund's McKnight Doctoral Fellowship, Alfred P. Sloan Minority Ph.D. program, and the National GEM Consortium. Her professional goals include obtaining a research career in the pharmaceutical/medical device industry, and mentoring talented students from the Caribbean who have aspirations of careers in science and engineering.